

Review

A Brief History of Photoactive Interlocked Systems Assembled by Transition Metal Template Synthesis

Vitor H. Rigolin, Liniquer A. Fontana and Jackson D. Megiatto, Junior *

Institute of Chemistry, University of Campinas (UNICAMP), P.O. Box 6154, Campinas 13083-970, Brazil; vitorrigolin@gmail.com (V.H.R.); liniquerfontana@hotmail.com (L.A.F.)

* Correspondence: jdmj@unicamp.br

Abstract: More than three decades of research efforts have yielded powerful methodologies based on transition metal template-directed syntheses for the assembly of a huge number of interlocked systems, molecular knots, machines and synthesizers. Such template techniques have been applied in the preparation of mechanically linked electron donor–acceptor artificial photosynthetic models. Consequently, synthetic challenging photoactive rotaxanes and catenanes have been reported, in which the chromophores are not covalently linked but are still associated with undergoing sequential energy (EnT) and electron transfer (ET) processes upon photoexcitation. Many interlocked photosynthetic models produce highly energetic, but still long-living charge separated states (CSS). The present work describes in a historical perspective some key advances in the field of photoactive interlocked systems assembled by transition metal template techniques, which illustrate the usefulness of rotaxanes and catenanes as molecular scaffolds to organize electron donor–acceptor groups. The effects of molecular dynamics, molecular topology, as well as the role of the transition metal ion used as template species, on the thermodynamic and kinetic parameters of the photoinduced energy and electron transfer processes in the interlocked systems are also discussed.



Citation: Rigolin, V.H.; Fontana, L.A.; Megiatto, J.D., Junior. A Brief History of Photoactive Interlocked Systems Assembled by Transition Metal Template Synthesis. *Photochem* **2021**, *1*, 411–433. <https://doi.org/10.3390/photochem1030025>

Academic Editor: Stefanie Tschierlei

Received: 24 September 2021

Accepted: 14 October 2021

Published: 21 October 2021

Publisher's Note: MDPI stays neutral with regard to jurisdictional claims in published maps and institutional affiliations.



Copyright: © 2021 by the authors. Licensee MDPI, Basel, Switzerland. This article is an open access article distributed under the terms and conditions of the Creative Commons Attribution (CC BY) license (<https://creativecommons.org/licenses/by/4.0/>).

Keywords: artificial photosynthesis; mechanical bond; template synthesis

1. Introduction

The mechanical bond is defined as an entanglement in space between two or more component parts, such that they cannot be separated without breaking or distorting chemical bonds between atoms. One of the most interesting features of interlocked systems is that the mechanical bond restricts the degrees of freedom of the molecular components when compared to a mixture of the molecules in solution. Therefore, molecular dynamics can be better controlled in interlocked systems, very often through external stimuli, to yield relatively simpler dynamic systems that show emergent properties. Accordingly, the exploration of the dynamic properties in molecular interlocked systems through control of the relative motions of the mechanically linked molecular components has led to major advances in several scientific endeavors as well as to the development of the most popular and Nobel Laureate-producing research field of molecular machines [1–8].

The impressive advancements in the field of mechanically linked molecules we are now witnessing have been possible due to the development of reliable synthetic protocols to assemble interlocked systems in the early 1980s. The formation of mechanical bonds is thermodynamically prohibitive due to the large entropic penalty involved in the self-assembly of the molecular components dissolved in solution into the relatively higher-organized interlocked systems. To overcome such entropic costs, the formation of mechanical bonds requires template synthetic techniques, which are based on molecular recognition through formation of attractive secondary interactions between the molecular components in solution. Secondary interactions yield enthalpic gains, which can eventually overcome the entropic hurdles to drive the self-assembly of the molecular components into the specific molecular architectures that favor formation of mechanical bonds. Accordingly,

hydrogen bonding, π - π stacking, hydrophobic interactions, ion- and radical-pairing have been largely explored as template routes for molecular recognition and development of several efficient and elegant synthetic template techniques to afford interlocked systems. The prime examples of interlocked systems are rotaxanes (a dumbbell shaped molecular component in which a molecular ring is trapped) and catenanes (two or more interlocked rings) [1,9–15].

Among the template synthetic techniques published in the literature, the so-called transition metal template methodologies, which are based on the formation of coordinative bonds between functionalized ligands and transition metal ions as template species, have proven to be a powerful tactic to prepare molecular racks, ladders, squares, grids, cylinders, molecular boxes, knots and double-, triple-, and circular helicates, as demonstrated by Saalfrank [16,17], Lehn [9] and others [18]. In the field of interlocked molecules, this approach is best illustrated using Sauvage's pioneering and elegant 1,10-phenanthroline-copper(I) metal template strategy as example for the synthesis of catenanes (Figure 1) [19]. In this approach, the Cu(I) metal template ion gathers and positions the 2,9-diphenyl-1,10-phenanthroline bidentate ligands (phen) to form an entwined $[\text{Cu}(\text{phen})_2]^+$ complex through formation of coordinative bonds. As elegantly demonstrated by Schmittel [20,21], the formation of secondary π - π attractive interactions between the phenyl rings and the phen moieties provide the entwined $[\text{Cu}(\text{phen})_2]^+$ complex with extra stability and thereby are critical for the success of Sauvage's catenane metal template synthesis. Accordingly, the distorted tetrahedral geometry of the resulting $[\text{Cu}(\text{phen})_2]^+$ complex forces the phen ligands to physically overlap, which in turn creates the cross-over point that directs the hydroxyl groups on the phen ligands to point in opposite directions. Furthermore, the proximity of the hydroxyl groups in the entwined $[\text{Cu}(\text{phen})_2]^+$ complex favors the intramolecular macrocyclization Williamson reactions to afford catenanes, rather than deleterious intermolecular process that would yield oligomers and/or higher cyclic species. The removal of the Cu(I) template ion at the final step yields the target catenane [5,8,19]. As we shall see later, the strategy is easily adapted to the synthesis of rotaxanes. Later, Leigh and collaborators published a series of influential studies, which include other transition metal ions as template species, which have established the guidelines for diverse synthetic strategies and tactics to efficiently assemble rotaxanes, catenanes, molecular knots and higher order links via the formation of complexes with several geometries [22].

The elegant developments in the template synthesis of interlocked molecules and further exploration of the interesting dynamic properties of the mechanically linked systems that followed Sauvage's pioneering works attracted the attention of the scientific community working on artificial photosynthetic models [23–31]. The possibility to introduce mechanical bonds into electron donor–acceptor systems (D-A) opened the door to design structurally more complex D-A models in which the effects of molecular dynamics and molecular topology on the thermodynamic and kinetics of forward (ET) and back electron transfer (BET) reactions could be investigated. Many mechanically linked D-A systems assembled via template methodologies based on the formation of several secondary interactions have been published in the literature [32–52]. However, the transition metal template technique has become the most popular one as it offers an extra advantage over the other template techniques, namely the entwined metal complexes necessary to assemble the interlocked systems can also function, in most cases, as electronic relays [29,53–55].

In this context, we describe herein a brief overview of mechanically linked artificial photosynthetic models assembled by transition metal template techniques. There are a significant number of D-A interlocked photoactive systems reported in the literature that have been prepared from template synthetic methodologies based on the formation of secondary interactions other than coordinative bonds. Those works are beyond the scope of this account. The text is organized in a historical perspective, briefly describing the synthetic strategies to assemble the photoactive interlocked systems, followed by a discussion of their photophysical properties. The present text is by no means a review of the field, but rather a short account with illustrative examples of key advances in the

field. For extensive reviews, we direct the reader to several excellent works that have been published in the literature [1,24,31,36,56–58].

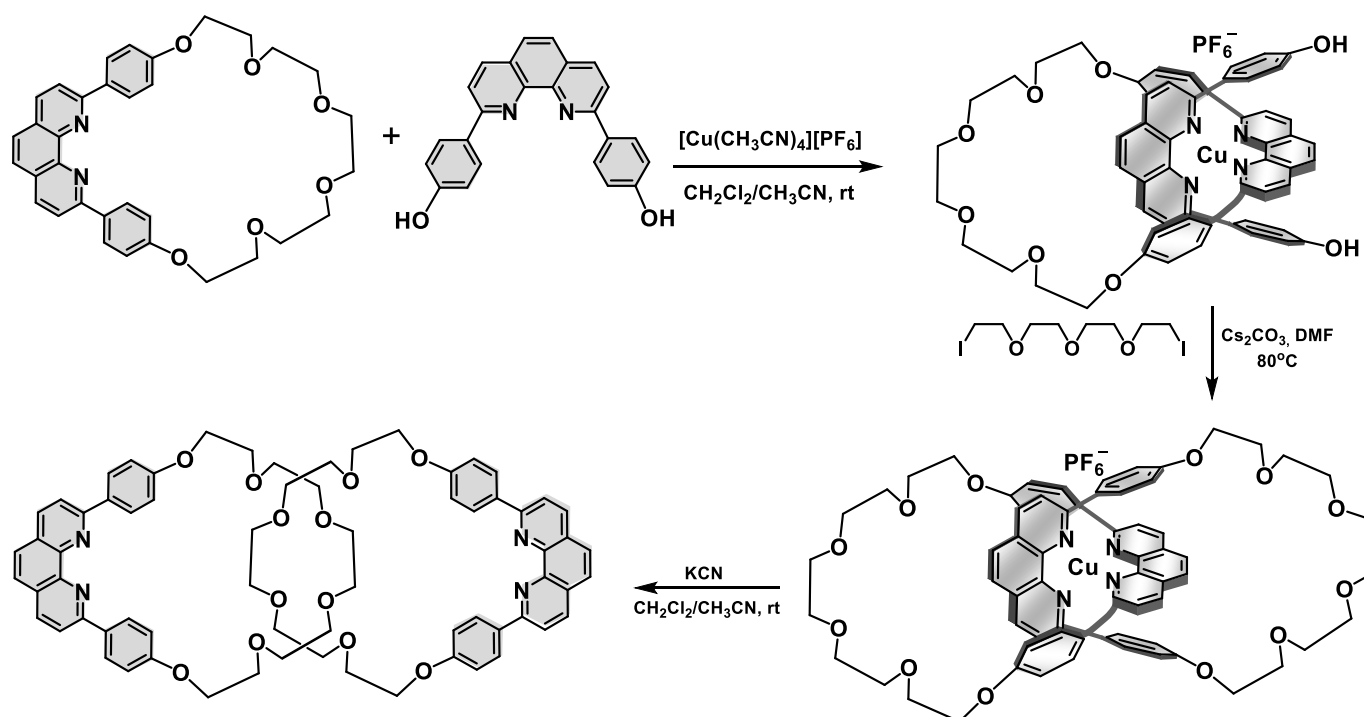


Figure 1. Original Sauvage Cu(I) ion template synthesis of catenanes. Formation of the entwined $[\text{Cu}(\text{phen})_2]^+$ complex, which is also stabilized by π - π secondary interactions between the phenyl rings and the phen moieties (represented as dashed lines), is quantitative. Subsequent ring closure by Williamson ether synthesis followed by removal of the Cu(I) template ion with KCN affords the target catenanes in 42% yield.

2. Interlocked Photosynthetic Models Decorated with Porphyrins as Electron Donors and Acceptors

Sauvage's group was the first to realize the potential of investigating rotaxanes and catenanes as interactive scaffolds to organize electron donor–acceptor moieties in artificial photosynthetic models. In their pioneering works [59–69], a large family of photoactive rotaxanes was synthesized and their photophysical properties were investigated. To illustrate Sauvage's pioneering works, the synthesis, dynamic and photophysical properties of rotaxane **1** will be discussed here (Figure 2) [59–61]. Rotaxane **1** was designed to have a cationic Au(III)porphyrinate group (AuP) as the electron acceptor, which was covalently attached to the ring component of the rotaxane, while the two Zn(II)porphyrinate stoppers (to prevent dissociation of the rotaxane upon removal of the Cu(I) template ion) were the electron donors. The synthesis of rotaxane **1** was achieved from an adaptation of the original Cu(I)-metal template synthetic strategy (Figure 1) and relied on the “gathering and threading” effects promoted by the Cu(I) ion template. Accordingly, a dialdehyde phen-based stringlike fragment was threaded through a previously prepared phen-containing ring with the appended AuP group to quantitatively form the entwined $[\text{Cu}(\text{phen})_2]^+$ complex that is also called pseudorotaxane. Finally, the two ZnP units were prepared simultaneously by reaction between the aldehyde functionalities on the thread component of the pseudorotaxane and dipyrromethane under acidic conditions (17% yield), followed by metalation of the free-base porphyrins with $\text{Zn}(\text{OAc})_2$, to afford rotaxane **1** (82% yield).

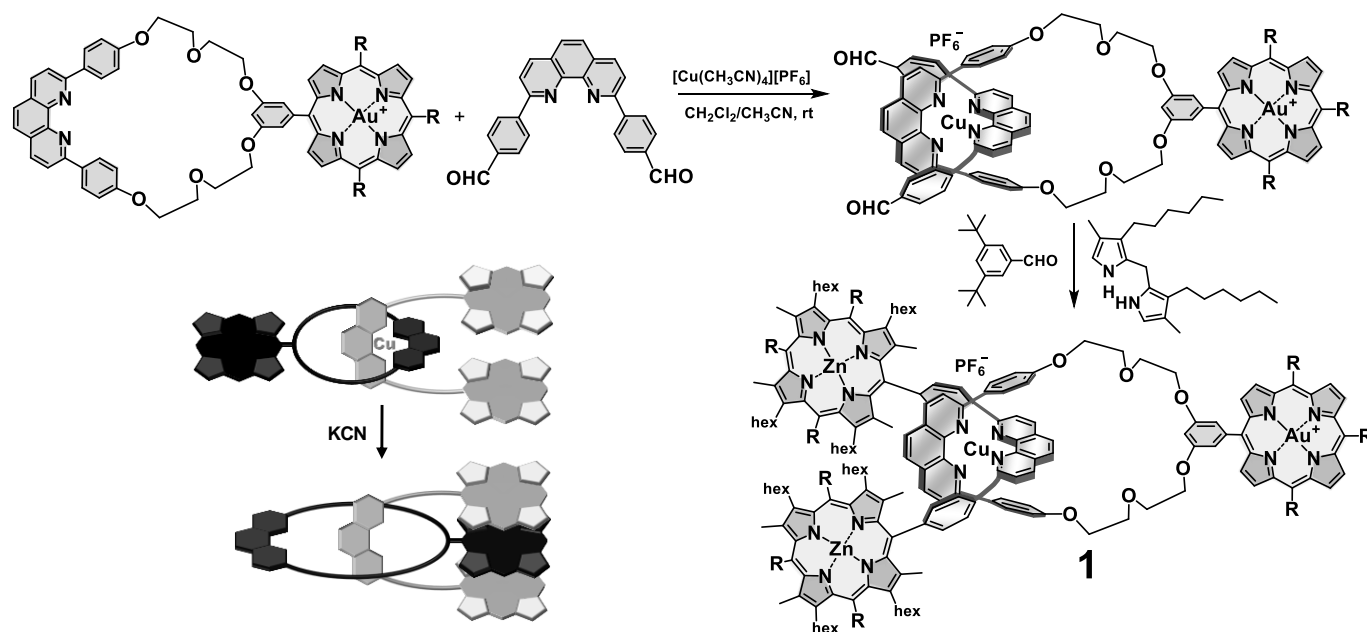


Figure 2. Sauvage's synthetic strategy to assemble photoactive rotaxane **1** and schematic representation of the rotaxane conformational change upon demetallation. R = 3,5-di-*tert*-butylphenyl groups; hex = hexyl aliphatic chains. In the schematic representation, the AuP moiety is in black and the ZnP stoppers are in gray.

Photophysical investigation of rotaxane **1** revealed that excitation of the ZnP chromophores yielded the corresponding singlet state ($^1\text{ZnP}^*$), which partially decayed by ET (70% yield, $k = 1.6 \times 10^{10} \text{ s}^{-1}$) to the AuP acceptor and 30% involving energy transfer (EnT) to the $[\text{Cu}(\text{phen})_2]^+$ complex ($k = 3.3 \times 10^9 \text{ s}^{-1}$). The resulting $\text{ZnP}^{\bullet+}-[\text{Cu}(\text{phen})_2]^+-\text{AuP}^\bullet$ charge separated state (CSS) afforded from the ET was found to biexponentially decay with lifetimes within 10–40 ns via BET. The biexponential decay of the CSS informed that rotaxane **1** was conformationally flexible, which allowed the photoactive subunits to have distinct electronic couplings. Exclusive excitation of the AuP moiety in **1** yielded the $^1\text{AuP}^*$, which was reductively quenched by the ZnP moieties via ET mediated by the $[\text{Cu}(\text{phen})_2]^+$ complex to afford the same $\text{ZnP}^{\bullet+}-[\text{Cu}(\text{phen})_2]^+-\text{AuP}^\bullet$ CSS [60–68].

Technically speaking, rotaxane **1** does not bear a mechanical bond, as the rigid tetrahedral metal chelate prevents the rotaxane components from undergoing the relatively long-range molecular motions about each other. Therefore, the authors removed the Cu(I) template ion by treating **1** with an excess of KCN to investigate the possible rearrangements of the chromophores in the Cu-free rotaxane. From a detailed spectroscopic investigation by NMR techniques, it was demonstrated that upon demetallation of **1**, the ring component circumrotated about the thread to position the AuP group between the tweezers-like configuration of the ZnP stoppers. This dynamic process was driven by attractive π - π interactions between the chromophores, which yielded the most stable ZnP-AuP-ZnP triple decker molecular configuration, schematically shown in Figure 2 [62]. However, due to the proximity of the chromophores in the Cu-free rotaxane, many intermediates produced upon photoexcitation had too short lifetimes to be investigated in the timeframe of the available spectrometers (20 ps), thus precluding a detailed investigation of the photophysical properties of the demetallated rotaxanes. Despite those limitations, Sauvage and coworkers have demonstrated for the first time that the inherent dynamic processes brought by mechanical bonds could be used to rearrange the photoactive subunits in rotaxanes to completely change the kinetics of ET and BET. The same group also reported a series of similar multirotaxanes and the parent catenanes, whose syntheses and photophysical properties have already been reviewed [57,69].

3. Interlocked Photosynthetic Models Decorated with Porphyrins as Electron Donors and Fullerenes as Acceptors

The pioneering works by Sauvage and collaborators brought much insight into the effects of molecular topology on the thermodynamics and kinetics of photo-induced processes. However, in addition to the already mentioned ultrafast ET and BET processes of the ZnP-AuP-based rotaxanes and catenanes, another limitation found in those pioneering works was the overlapping of the spectroscopic signals of the many intermediates formed upon excitation. Accordingly, a complete determination of the kinetic parameters for the expected photophysical decays was impossible. The solution to this problem was to replace the AuP acceptor with [60]fullerene (C_{60}) in the interlocked molecular architectures. This idea came from the vast experimental evidence accumulated from the investigations of covalently linked D-A photoredox arrays published in the literature [70–78]. Such works clearly demonstrated that C_{60} was a superior electron acceptor than AuP and other chromophores commonly used in artificial photosynthetic models at that time, such as quinones [79]. Those studies confirmed that the C_{60} rigid structure associated with its poor solvation yielded small values of reorganization energy (λ), which shifted the wasteful BET processes into the inverted region of the Marcus parabolic relationship between free energy change of the ET processes and λ [80]. Accordingly, long-lived CSSs in many covalently linked artificial photosynthetic models containing C_{60} as acceptors were reported. Furthermore, the transient absorption spectroscopic signature of the reduced fullerene radical anion ($C_{60}^{\bullet-}$) appears at about $\lambda_{\max} \approx 1000$ nm, which is usually a clean region of the absorption spectrum, thereby solving the signal overlapping issues in previous photophysical investigations [70,71].

Sauvage in collaboration with Diederich and Nierengarten reported the first rotaxane containing C_{60} as the electron acceptor. In their design, the rotaxane was assembled via the Cu(I) metal template technique and the C_{60} groups functioned as stoppers in the interlocked photoactive model (Figure 3a) [81]. The synthetic strategy used to prepare target *bis*- C_{60} -rotaxane **2**, which was isolated in 15% yield, was based on Hay oxidative alkyne–alkyne coupling to introduce the fullerene groups into the $[Cu(phen)_2]^+$ pseudorotaxane. The non-interlocked thread compound shown in Figure 3a was also isolated from the crude product, thus informing that the central $[Cu(phen)_2]^+$ complex in the pseudorotaxane partially dissociated during the Hay-stoppering reactions. Investigation of the redox properties of rotaxane **2** revealed a significant anodic shift (~ 0.2 V) for the reversible oxidation of the $[Cu(phen)_2]^+$ complex (0.87 eV vs. SCE) in comparison with a reference compound (0.68 eV vs. SCE) lacking the fullerene groups. Reduction (irreversible) of the C_{60} component appeared in the typical range (0.6 eV vs. SCE), leading the authors to speculate that the strong electron-withdrawing effect of the fullerenes might substantially destabilize the highest oxidation state of the $[Cu(phen)_2]^+$ complex [82].

Time-resolved spectroscopic investigation revealed that excitation of rotaxane **2** at 355 or 532 nm simultaneously yielded the metal-to-ligand charge transfer (MLCT*) in the $[Cu(phen)_2]^+$ complex (40% yield) and the $^1C_{60}^*$ (60% yield) excited states (step 1, Figure 3b). The authors proposed that the $^1C_{60}^*$ decayed via energy transfer (EnT) to the $[Cu(phen)_2]^+$ complex (62% yield, $k = 1.6 \times 10^9$ s $^{-1}$, step 2) in competition with intersystem crossing (28% yield, $k = 6.2 \times 10^8$ s $^{-1}$ to generate $^3C_{60}^*$, step 3). From the electrochemical measurements, both MLCT* and $^1C_{60}^*$ should have decayed via ET to form the $[Cu(phen)_2]^{2+}-C_{60}^{\bullet-}$ CSS (steps 4 and 5). A weak transient absorption signal at 740 nm with a lifetime of 1.7 μ s was observed, which could have been attributed to formation of the $[Cu(phen)_2]^{2+}-C_{60}^{\bullet-}$ CSS. However, the unusually long lifetime of this transient species along with the impossibility of observing the spectroscopic signature of the $C_{60}^{\bullet-}$ radical anion around $\lambda = 1000$ nm due to instrumental limitations led the authors to conservatively conclude that the $[Cu(phen)_2]^{2+}-C_{60}^{\bullet-}$ CSS was probably formed in rotaxane **2**, but BET (step 8) was too fast to allow unambiguous detection of the expected $[Cu(phen)_2]^{2+}-C_{60}^{\bullet-}$ CSS [82].

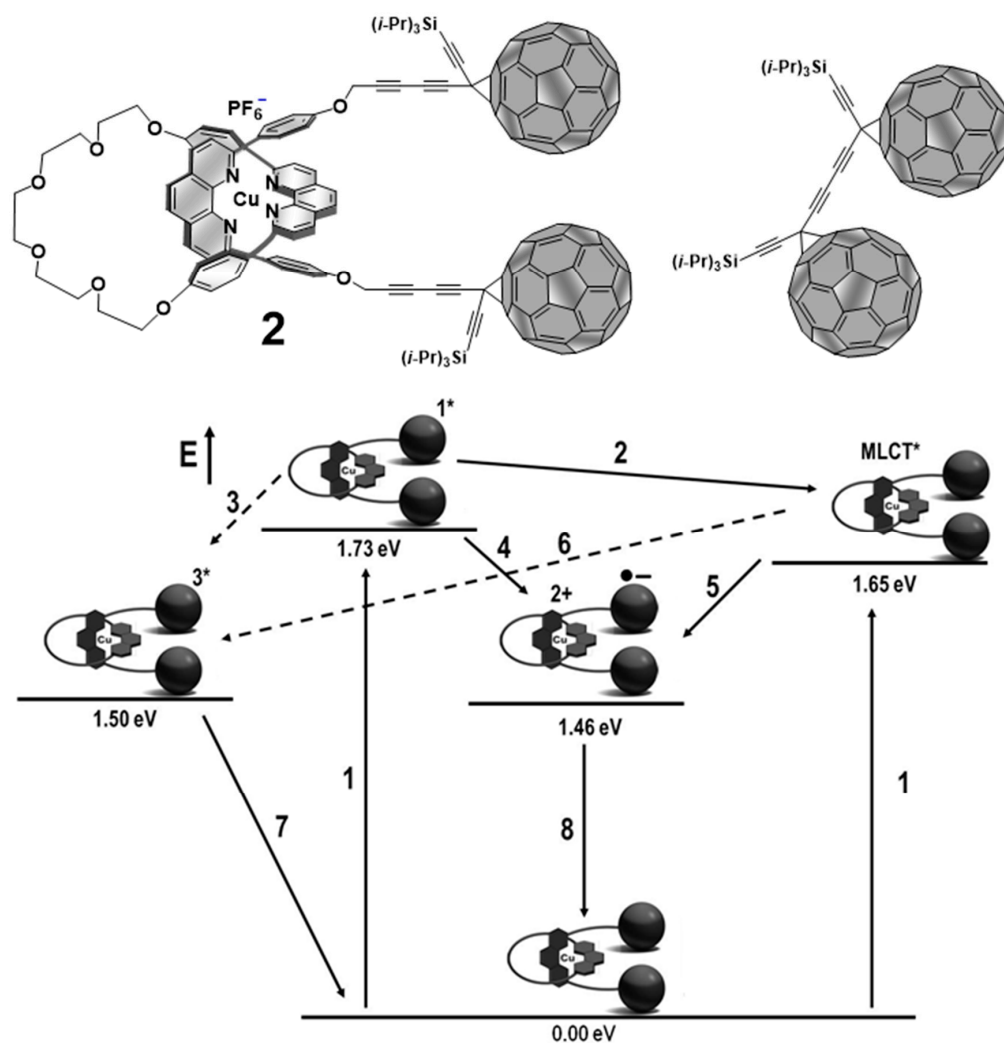


Figure 3. (a) First rotaxane structure bearing fullerenes subunits prepared by Sauvage, Diederich and Nierengarten. The C_{60} -dimer byproduct was also isolated from the final stopping reaction. *i*-Pr = isopropyl group. (b) Energy level diagram and proposed photophysical decay pathways for rotaxane **2** upon excitation at 355 or 532 nm. Dashed arrows show intersystem crossings.

Based on those previous works, Schuster's and Guldi's groups initiated a research program to further improve the synthetic methodologies to prepare Sauvage-type interlocked systems containing C_{60} as electron acceptor, while overcoming the instrumental limitations that had prevented the complete elucidation of photo-induced processes in the rotaxanes and catenanes. In their initial efforts [83], Schuster and colleagues elaborated elegant synthetic strategies to afford a new family of $[Cu(phen)_2]^+$ -based rotaxanes, in which the ZnP electron donors were positioned at the end of the phen-thread component, while the C_{60} acceptor was covalently attached to the phen-macrocycle (Figure 4) using classical fullerene chemistry [73].

Schuster's synthetic strategies were conceived to minimize the usual C_{60} solubility issues and the inherent kinetic lability of the coordinative bonds that held together the $[Cu(phen)_2]^+$ complex. Accordingly, the new family of photoactive rotaxanes were prepared following a stepwise approach. For illustrative purposes, the synthesis of rotaxane **3** will be described (Figure 5). Starting with phen-macrocycle **6**, the malonate synthon reacted smoothly with C_{60} under Bingel–Hirsch conditions [73] to yield compound **7**, which was soluble in most organic solvents. The mono-ZnP-stoppered thread **10** was prepared from tetraarylporphyrin carboxylic acid **8** and phen-thread **9** via esterification reaction using dicyclohexylcarbodiimide (DCC) as coupling agent and 4-dimethylaminopyridine

(DMAP) as catalyst. The “threading” reaction of the mono-ZnP-stoppered phen-stringlike fragment **10** through macrocycle **7** was accomplished using the Cu(I) ion as the template species to yield the $[\text{Cu}(\text{phen})_2]^+-\text{C}_{60}$ pseudorotaxane precursor **11**, which was known to be less prone to dissociation [17], thereby yielding rotaxanes in larger yields. In the final step, a second DCC/DMAP ester-coupling reaction between pseudorotaxane **11** and tetraarylporphyrin carboxylic acid **8** afforded target rotaxane **3** in about 40% yield.

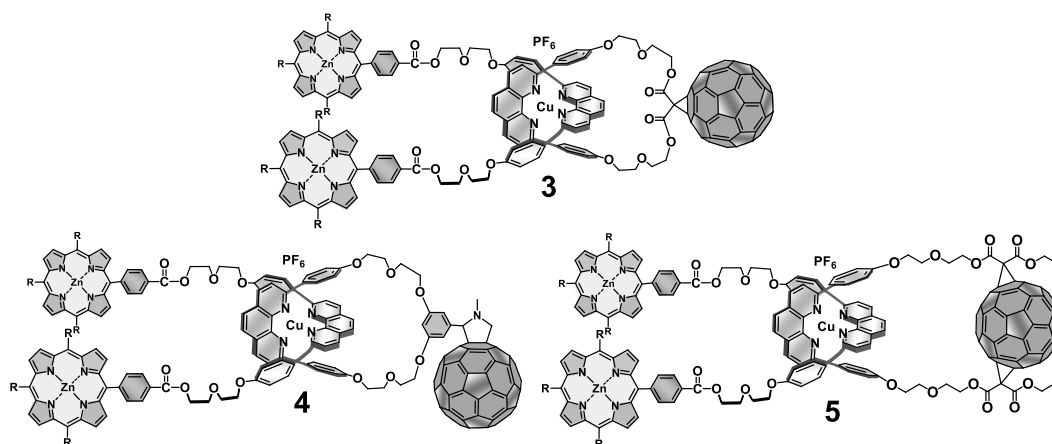


Figure 4. Schuster’s photoactive rotaxanes assembled via the Cu(I)-directed metal template synthesis and decorated with ZnP and C_{60} groups as electron donors and acceptor, respectively. Lifetimes of the final $\text{ZnP}^{*\bullet+}-[\text{Cu}(\text{phen})_2]^+-\text{C}_{60}^{\bullet-}$ CSSs in rotaxanes **3**, **4** and **5** were 0.49, 1.40 and 0.51 μs , respectively.

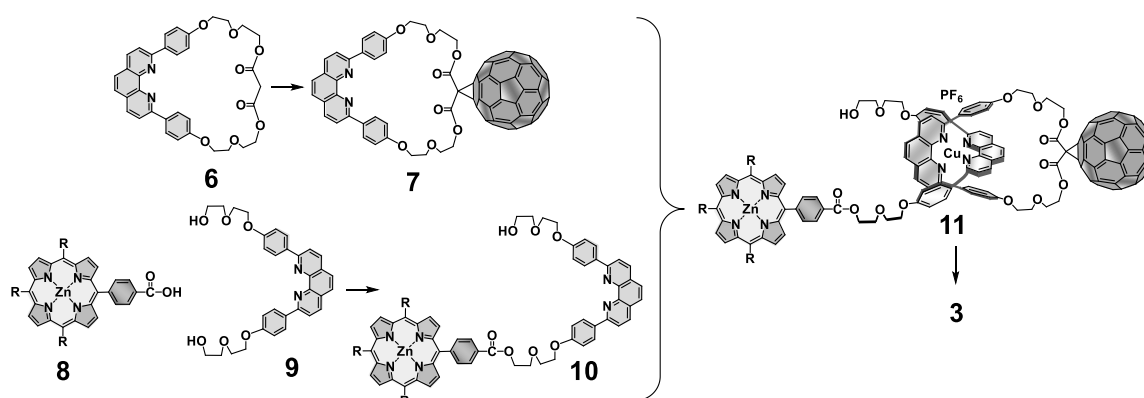


Figure 5. Stepwise synthetic strategy developed by Schuster and coworkers to assemble rotaxane **3**.

An elegant series of electrochemical, time-resolved emission and transient absorption experiments was then carried out on the new family of rotaxanes and related model compounds by Echegoyen’s and Guldi’s groups. Such detailed investigation enabled the authors to unambiguously assign the specific roles of each entity in the rotaxanes, thereby allowing the determination of the kinetics of the photoinduced processes in the interlocked molecules (Figure 6). Exclusive excitation of the ZnP subunits at 420 nm yielded the $^1\text{ZnP}^*$ excited state (step 1), which was moderately quenched (the fluorescence lifetimes of the $^1\text{ZnP}^*$ were 3.2 ns in the reference compound and 1 ns in the rotaxanes). Furthermore, the emission quenching was independent of the solvent polarity and present in rotaxane model compounds lacking the fullerene moiety, which informed the authors that the quenching did not involve direct interaction of $^1\text{ZnP}^*$ and C_{60} . Accordingly, the authors attributed the quenching to EnT from the $^1\text{ZnP}^*$ to the $[\text{Cu}(\text{phen})_2]^+$ subunit to yield the corresponding MLCT* excited state (step 2). By monitoring the transition absorption signal of the $\text{C}_{60}^{\bullet-}$ at around $\lambda_{\text{max}} = 1000$ nm in the rotaxanes, which obeyed a biexponential rate law, along with a careful transient absorption investigation of several model compounds, the authors

determined that the MLCT* manifold was oxidatively quenched by the C₆₀ via ET to yield the intermediate ZnP–[Cu(phen)₂]²⁺–C₆₀^{•−} CSS, which partially yielded the ground state via BET (steps 3 and 5, respectively). However, detection of the strong signature transient absorption of the ZnP^{•+} centered at λ_{max} = 680 nm, whose lifetime matched the long component decay observed for the biexponential rate law of the fingerprint absorption of the C₆₀ at λ_{max} = 1040 nm, provided clear cut evidence for an ET reaction from the ZnP stoppers to the oxidized [Cu(phen)₂]²⁺ complex to afford the final ZnP^{•+}–[Cu(phen)₂]⁺–C₆₀^{•−} CSS (step 4). The lifetimes of the final CSSs in the rotaxanes were in the range of 0.4–1.4 μs (step 6). Such relatively long lifetimes of the final CSSs allowed the authors to conclude that BET in the rotaxanes occurred in the Marcus inverted region. The main photophysical decay of Schuster's and Guldi's rotaxanes are summarized in the energy level diagram depicted in Figure 6.

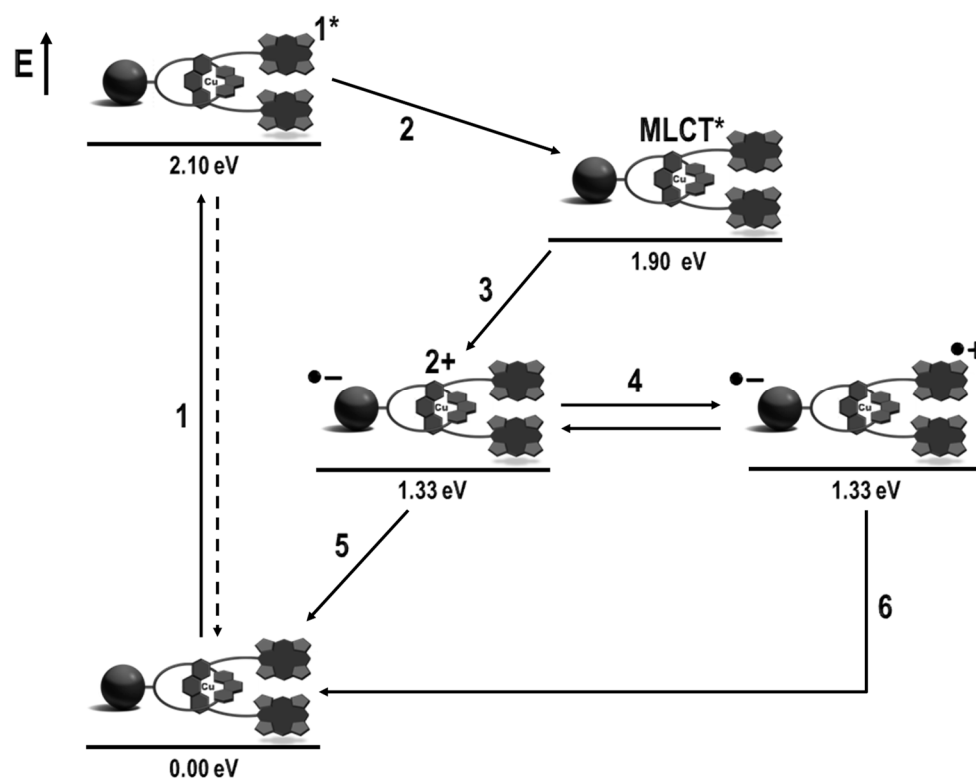


Figure 6. Energy level diagram and proposed photophysical decay pathways for Schuster-Guldi rotaxanes upon exclusive excitation of the ZnP groups at 420 nm.

Based on those promising findings, Schuster, Guldi and collaborators reported a second set of rotaxanes [84], in which the positions of the ZnP and C₆₀ groups were reversed. Accordingly, in this new set of rotaxanes, the ZnP moiety was covalently attached to the macrocycle component of the rotaxane, while the fullerenes acted as stoppers on the thread. Following a similar stepwise strategy, rotaxanes 12–14 were assembled (Figure 7) and their interlocked structures confirmed by NMR spectroscopic investigation. The overall sequence of photophysical events in the fullerene-stoppered rotaxanes was identical to that shown in Figure 6, thereby confirming the assignments of the role of each photoactive subunit in the rotaxanes. However, the lifetimes of the final ZnP^{•+}–[Cu(phen)₂]⁺–C₆₀^{•−} CSSs were much longer for the second set of rotaxanes, particularly that observed for rotaxane 12, which was 32 μs in THF and was among the longest ever reported for the CSS state of a simple porphyrin–fullerene dyads at the time. The authors suggested that such distinctly lifetimes observed for their D-A rotaxanes could be due to a variety of factors, including D-A distance, the chemical nature of the linker between the chromophores, and effects of molecular topology on the kinetics of the photoinduced processes [85].

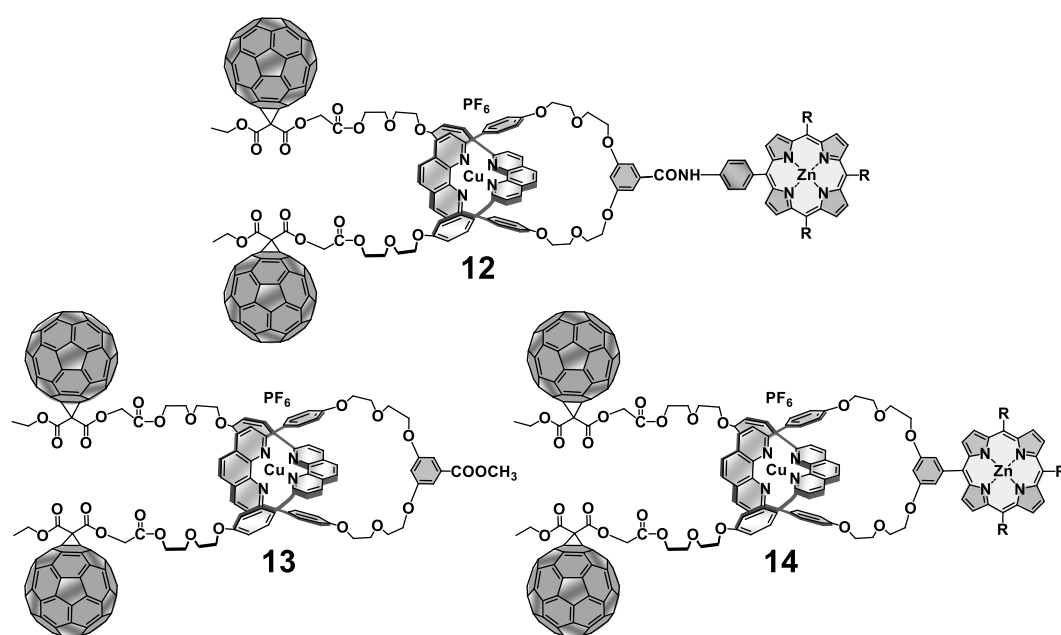


Figure 7. Schuster-Guldi second generation of photoactive rotaxanes assembled via the Cu(I)-directed metal template synthesis and decorated with ZnP and C₆₀ groups as electron donors and acceptor, respectively. Lifetimes of the final ZnP^{•+}–[Cu(phen)₂]⁺–C₆₀^{•–} CSSs in rotaxanes **12** and **14** were 32 and 29 μs, respectively. Rotaxane **13** was investigated as a rotaxane reference compound.

4. Effects of Molecular Topology on the Kinetics of Photoinduced Processes in Interlocked Molecules Decorated with Porphyrins as Electron Donors and Fullerenes as Acceptors

From the achievements described in the previous section, along with the increasing amount of experimental evidence reported in the literature for D-A rotaxanes assembled by different template techniques, it became clear that small structural modifications, such as variation of the size and shape of the ring and thread components, as well as the type of chemical linkages that connect the chromophores to the interlocked architectures, significantly affected the kinetics of the photoinduced processes. In other words, investigation of how molecular topology affected the ET and BET processes was of paramount importance in the field. In chemistry, molecular topology generally refers to molecules whose representations based on atoms and bonds are nonplanar. In chemical topology, a molecule can be distorted as much as one wants, but its topological properties are not modified as long as no cleavage of a chemical bond occurs. According to this definition, rotaxanes and catenanes are topologically different. For example, in a [2]catenane, the two mechanically linked rings are topologically distinct from the two molecular rings that are not interlocked. Therefore, catenanes are nontrivial topological systems. Conversely, a [2]rotaxane is topologically identical to its component parts as the ring can be separated from the thread by stretching or compressing the appropriate chemical bonds [1,4].

In this context, the best way to investigate the effects of molecular topology on the kinetics of the photoinduced processes was to synthesize rotaxanes and catenanes with identical molecular parameters and decorated with ZnP and C₆₀ chromophores. Although Schuster and coworkers demonstrated that ester-coupling reactions were suitable synthetic methodologies for the preparation of ZnP–C₆₀ rotaxanes, they failed in the preparation of the analogous catenanes. To overcome the synthetic challenges in the preparation of photoactive catenanes, Megiatto and Schuster developed an innovative synthetic strategy (Figure 8) based on “click reactions” [86,87] as the final step that transforms the [Cu(phen)₂]⁺-based pseudorotaxane **17** into target rotaxane **18** (via stoppering reactions using **15**) and catenane **19** (via macrocyclization reactions using **16**). For the success of this strategy, the final “click reactions” had to occur fast in order to favorably compete with the

kinetic labile coordinative bonds that hold the components in the entwined configuration in pseudorotaxane **17**. Otherwise, a detrimental unthreading process via dissociation of the $[\text{Cu}(\text{phen})_2]^+$ complex would take place and the components would react in a random rather than in a templated fashion.

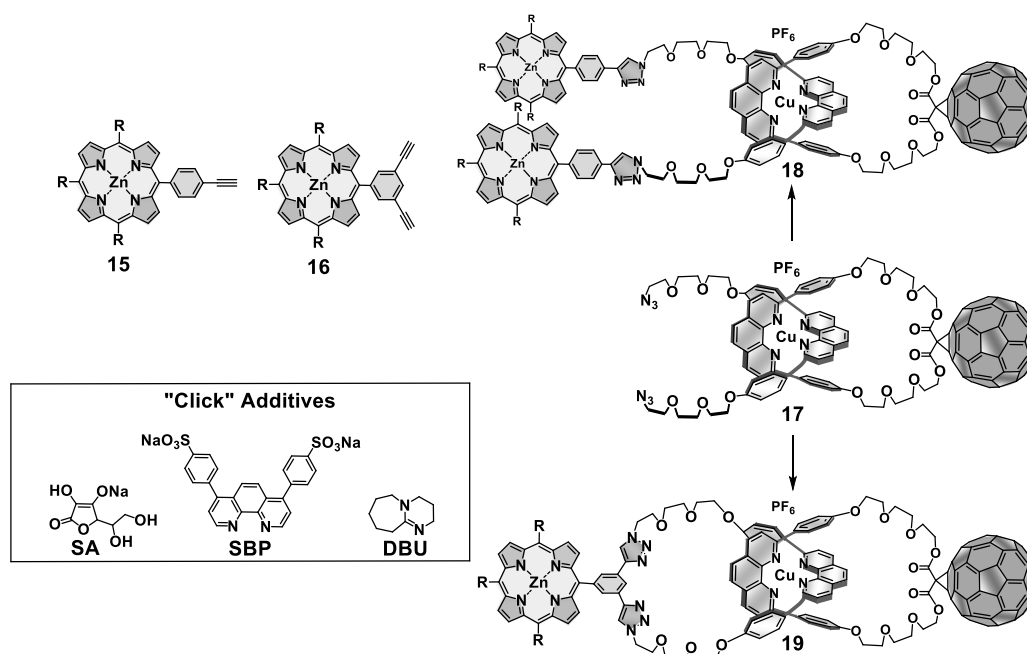


Figure 8. Synthetic strategy for the synthesis of rotaxanes and catenanes using the Cu(I)-template directed technique in combination with “click reactions”. R = 3,5-di-*tert*-butylphenyl groups located at the *meso* positions of the porphyrins, which are not shown for clarity purposes.

The hurdles of the proposed “click” synthetic strategy became obvious in the initial efforts. Classical tactics to improve the kinetics of a chemical reaction, such as increasing the concentration of the reactants and/or adding an excess of one of the reactants, worked well for the synthesis of rotaxane **18**, but completely failed when trying to prepare the analogous catenane **19**, as intractable product mixtures containing oligomers and polymers were afforded under those conditions. On the other hand, the typical homeopathic reactant dilution necessary for efficient macrocyclization reactions yielded target catenane **19**. However, such high-dilution conditions, when applied to the preparation of rotaxane **18**, led to very poor yields, most likely because the lower “click” reaction rates allowed dissociation of pseudorotaxane **17** in the route to rotaxane **18**.

To overcome those diverging reaction conditions and afford both rotaxanes and catenanes from the same experimental conditions, a new “click” catalyst brew was developed to speed up the final stoppering and macrocyclization reactions. The catalyst consisted of a mixture of copper(I)iodide, sodium ascorbate (SA), sulfonated bathophenanthroline (SBP) and 1,8-diaza-[5.4.0]bicycloundec-7-ane (DBU), all previously dissolved in a solvent mixture composed of $\text{H}_2\text{O}/\text{EtOH}$ (1:1, *v/v*). This highly active “click” catalyst, when added to a mixture of the proper building blocks and reactant stoichiometry dissolved in a $\text{CH}_2\text{Cl}_2/\text{CH}_3\text{CN}$ (7:3, *v/v*) organic solvent mixture, yielded rotaxane **18** and catenane **19** in respectable 75% and 57% yields, respectively. Most importantly, such an innovative synthetic approach allowed the preparation for the first time of interlocked D-A systems with the same molecular structural parameters. Therefore, the distinct molecular topology of catenanes and rotaxanes and its eventual effects in the photoinduced processes on the interlocked systems could be investigated [88–96].

A detailed electrochemical, steady-state and time-resolved absorption and emission investigation of rotaxane **18** and catenane **19**, as well as of several model compounds, was

carried out by Guldi's group to determine all thermodynamic and kinetic parameters of the photoinduced processes (Figure 9). Not surprisingly, the sequence of events following exclusive photoexcitation of the ZnP moieties in rotaxane **18** and catenane **19** at 420 nm was identical to that observed for the ester-linked rotaxanes described in the previous section: (1) EnT on the ns time scale from $^1\text{ZnP}^*$ to the $^3\text{MLCT}^*$ state of the $[\text{Cu}(\text{phen})_2]^+$; (2) ET from the $^3\text{MLCT}^*$ to C_{60} to give the intermediate $\text{ZnP}-[\text{Cu}(\text{phen})_2]^{2+}-\text{C}_{60}^{\bullet-}$ CSS; (3) ET from the ZnP to the oxidized $[\text{Cu}(\text{phen})_2]^{2+}$ complex to give the final long-distance $\text{ZnP}^{\bullet+}-[\text{Cu}(\text{phen})_2]^+-\text{C}_{60}^{\bullet-}$ CSS; (4) BET to regenerate the ground state [92,94]. This sequential ET processes were confirmed by electron paramagnetic resonance spectroscopy (EPR), in which the formation of both intermediate and final CSSs in rotaxane **18** (Figure 9a) and catenane **19** (Figure 9b) were detected [97,98].

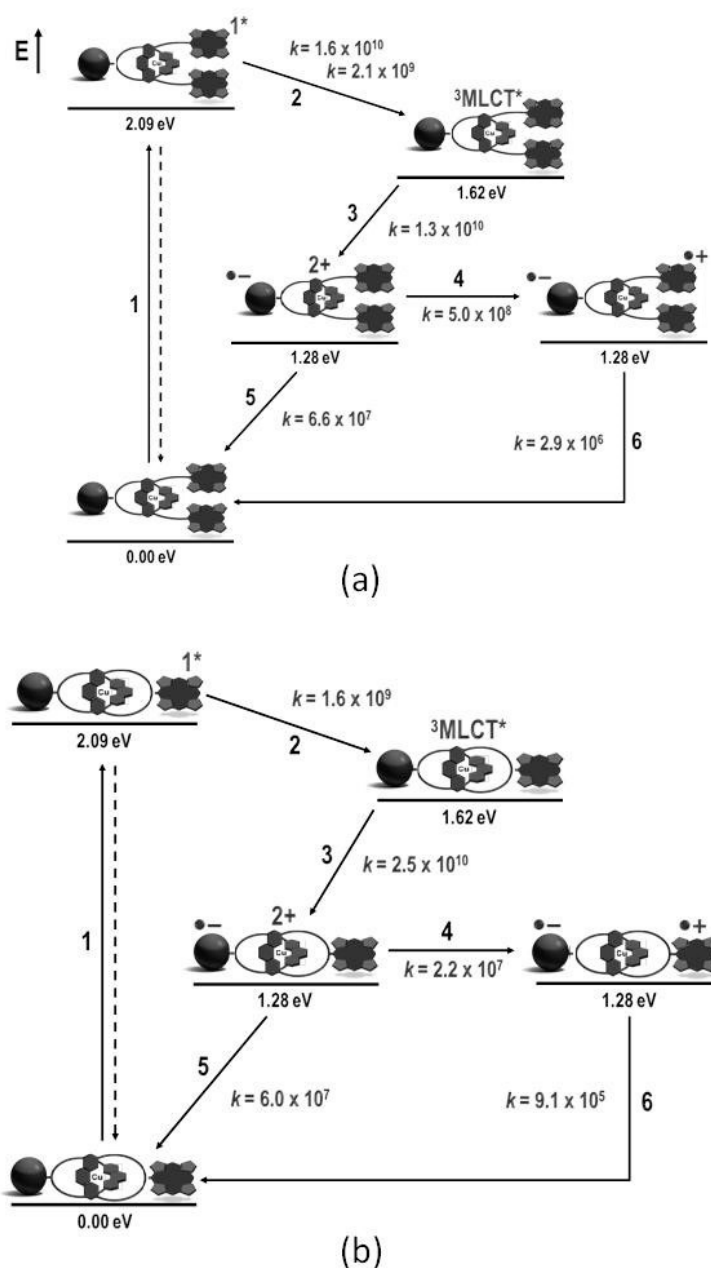


Figure 9. Energy level diagrams, proposed decay pathways, and rate constants in s^{-1} in benzonitrile following exclusive excitation of the ZnP moiety at 420 nm. (a) for rotaxane **18**. (b) for catenane **19**. Lifetimes of the final $\text{ZnP}^{\bullet+}-[\text{Cu}(\text{phen})_2]^+-\text{C}_{60}^{\bullet-}$ CSSs in rotaxanes **18** and **19** were 0.24 and 1.10 μs , respectively.

However, the effects of the distinct molecular topologies of the rotaxane and catenane became clear in the investigation of the dynamics of the photoinduced processes. The lifetime of the final $\text{ZnP}^{\bullet+}-[\text{Cu}(\text{phen})_2]^+-\text{C}_{60}^{\bullet-}$ CSS was $0.24 \mu\text{s}$ in rotaxane **18**, while it was $1.10 \mu\text{s}$ in catenane **19** under the same conditions. From time-resolved fluorescence experiments, it was observed that the $^1\text{ZnP}^*$ presented a biexponential decay with lifetimes of 61 ps and 400 ps for rotaxane **18**, while catenane **19** showed a monoexponential decay with a lifetime of 500 ps for the $^1\text{ZnP}^*$ excited state. Those findings informed that the ZnP stoppers in rotaxane **18** had distinctly electronic couplings with the other chromophores; therefore, they were at different distances from each other. A careful structural investigation by NMR spectroscopy revealed that rotaxane **18** was conformationally flexible and adopted a more compact structure in solution driven by secondary attractive π - π interactions between the chromophores. More specifically, one of the ZnP stoppers was closer to the $[\text{Cu}(\text{phen})_2]^+$ and C_{60} subunits, while the other was further away. On the other hand, structural analysis of catenane **19** informed that it adopted an extended conformation with the chromophores as far apart as possible. Computation simulations confirmed the folded and extended conformations adopted by rotaxane **18** and catenane **19**, respectively (Figure 10) [92–94].

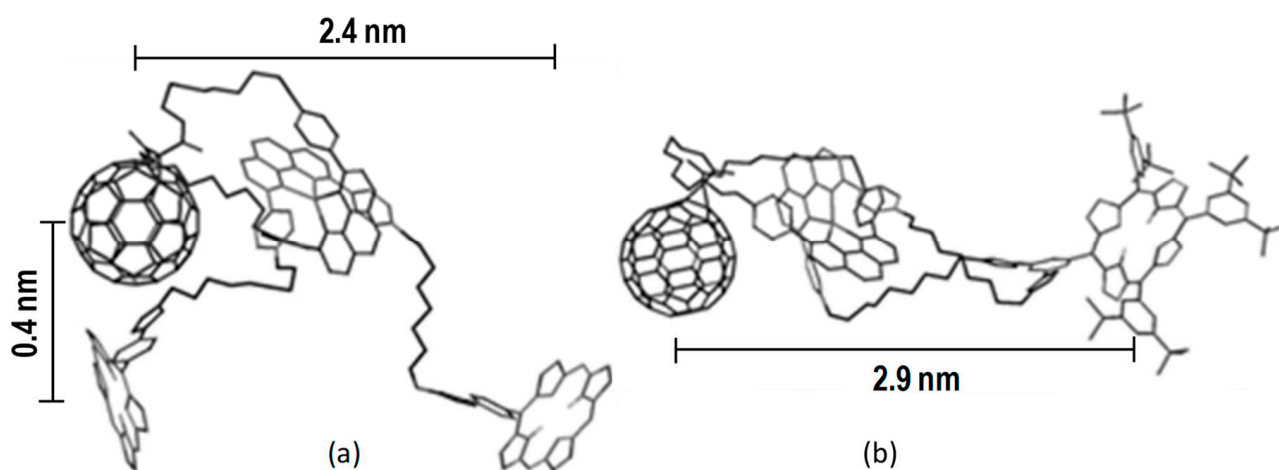


Figure 10. Computational molecular models (Spartan'06, PM3 minimization level): (a) rotaxane **18**; (b) catenane **19**. For clarity, the hydrogen atoms have been removed from the structure along with the 3,5-di-tert-butylphenyl groups on the *meso* positions of the porphyrins. The computed ZnP- C_{60} center-to-center distances are shown.

To provide further evidence that the distinct lifetimes for the final $\text{ZnP}^{\bullet+}-[\text{Cu}(\text{phen})_2]^+-\text{C}_{60}^{\bullet-}$ CSS were due to molecular topology, the authors investigated the photophysical properties of rotaxane **18** in the presence of 1,4-diazabicyclo [2.2.2]-octane (DABCO). The idea was to use formation of coordinative bonds between the ZnP stoppers and the bidentate DABCO ligand to disrupt the π - π interactions observed in **18** and, consequently, unfolding the rotaxane architecture to yield catenanelike structure **20** (Figure 11). Steady-state UV-Vis and fluorescence spectroscopic data revealed formation of the DABCO/ZnP complex with the expected 1:2 ratio, thereby confirming the expected transformation of rotaxane **18** into **20**. Time-resolved transient absorption experiments on **20** indicated a monoexponential decay for the $\text{ZnP}^{\bullet+}$ transient absorption at $\lambda_{\text{max}} = 680 \text{ nm}$ with a lifetime of $1.3 \mu\text{s}$, which matched the long component decay observed for the biexponential rate law found for the fingerprint absorption of the $\text{C}_{60}^{\bullet-}$ species at $\lambda_{\text{max}} = 1040 \text{ nm}$ (the shorter component was attributed to BET in the $\text{ZnP}-[\text{Cu}(\text{phen})_2]^{2+}-\text{C}_{60}^{\bullet-}$ intermediate CSS). Accordingly, the final $\text{ZnP}^{\bullet+}-[\text{Cu}(\text{phen})_2]^+-\text{C}_{60}^{\bullet-}$ CSS had virtually the same lifetime in **20** as in catenane **19**. Based on those findings, the authors concluded that the longer lifetime observed for the final $\text{ZnP}^{\bullet+}-[\text{Cu}(\text{phen})_2]^+-\text{C}_{60}^{\bullet-}$ CSS in catenane **19** was due to its more rigid structure, which kept the chromophoric subunits further apart, thus decreasing the electronic coupling of the radical ions when compared to that in the analogous but

more flexible rotaxane **18**. Thus, such extensive investigation clearly revealed, for the first time, the molecular topological effects on the dynamics of the photoinduced processes in interlocked molecules [94].

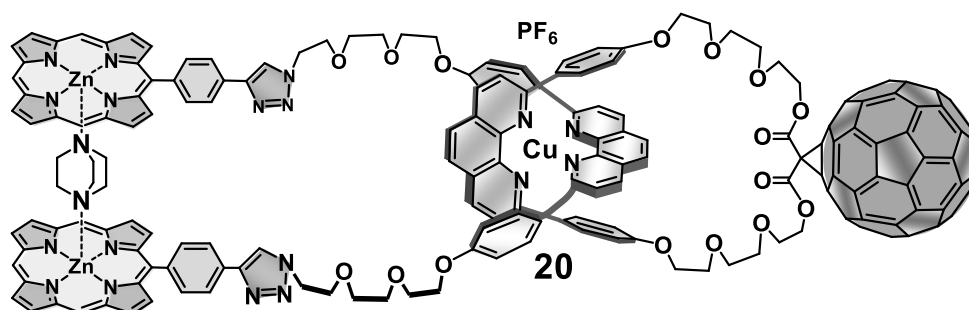


Figure 11. Structure of catenane-like **20** afforded from complexation of a DABCO molecule in between the two ZnP stoppers of rotaxane **18**. The 3,5-di-*tert*-butylphenyl groups located at the *meso* positions of the porphyrins are not shown for clarity purposes. Lifetime of the final $\text{ZnP}^{\bullet+}-[\text{Cu}(\text{phen})_2]^+-\text{C}_{60}^{\bullet-}$ CSSs in catenane-like structure **20** was 1.30 μs .

With those achievements, Schuster, Megiatto and Guldi focused their efforts to investigate the possibility of using the inherent circumrotation, shuttling, pirouetting and rocking motions of the entangled components to reposition the ZnP and C_{60} subunits in order to favor ET, while retarding the wasteful BET to afford CSSs with longer lifetimes. As demonstrated by Sauvage's works, one way to trigger intracomponent motions was removing the Cu(I) template ion from the central $[\text{Cu}(\text{phen})_2]^+$ complex [61]. However, the classical KCN treatment to remove the Cu(I) ion from Sauvage's interlocked systems [5,19] was incompatible with the fullerene-based counterparts. From MALDI-TOF experiments on the fullerene-containing interlocked molecules, it was found that although the CN^- anions removed the Cu(I) ions from the rotaxanes and catenanes, unfortunately, they also reacted with the fullerene based compounds via nucleophilic attack that led to multiple additions of CN^- anions to the carbon cage. To circumvent this synthetic issue, the authors developed a demetallation protocol using NH_4OH as the active reagent, which proved to be successful in removing the Cu(I) ion template from the interlocked systems with no side reactions with C_{60} [99].

Photophysical investigation of Cu-free rotaxane **21** (Figure 12a) yielded only ZnP and C_{60} triplet excited states upon exclusively excitation of either chromophore. No evidence for ET reactions was found, even in high polar solvents. That was a surprising result as it was expected that removal of the Cu(I) ion from the rotaxane would allow a higher degree of freedom for the chromophores to reposition themselves close together, driven by π - π attractive interactions between the ZnP and C_{60} groups. A structural investigation by NMR spectroscopy of rotaxane **21** was undertaken to identify the conformational changes brought by the removal of the Cu(I) template ion. As π - π interaction was thought to be the driving force of the conformational rearrangement, the shielding of specific protons in the rotaxane structure was used as a probe in the study. The NMR spectrum of **21** revealed that the protons of the phen-chelate on the ring component were shielded when compared to the analogous ones on the thread, thereby informing the researchers that the former were in the range of the ZnP magnetic anisotropy. Accordingly, the tweezerlike configuration of the ZnP stoppers in **21** favored formation of π - π attractive interactions with the planar phen moiety on the ring rather than with the spherical fullerene (Figure 12b), therefore preventing the expected pirouetting of the ring component about the thread. From the investigation, the authors demonstrated that removal of the Cu(I) template ion indeed promoted a conformational change in the rotaxanes; however, the resulting rearrangement of the chromophores did not improve the rates of the ET processes as originally thought, but rather shut them down completely [94]. On the other hand, the critical role of the

$[\text{Cu}(\text{phen})_2]^+$ complex as mediator in the electronic interactions between the ZnP and C_{60} groups in the interlocked molecules was confirmed [64–69,94].

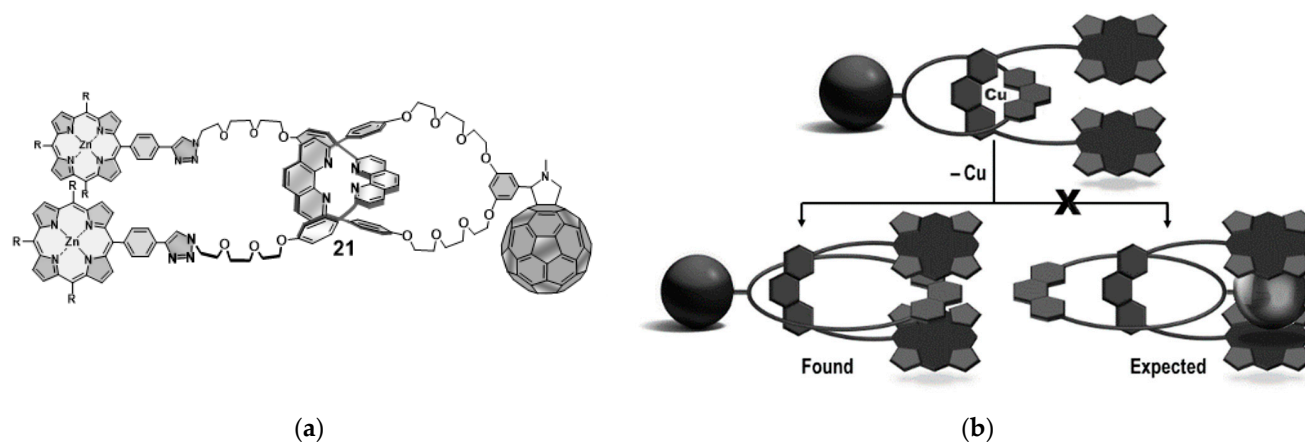


Figure 12. (a) Molecular structure of Cu-free rotaxane **21** and (b) schematic representation of the found and expected rotaxane conformational change upon demetallation as revealed by NMR investigation.

5. Multi-Chromophoric Rotaxanes as Artificial Photosynthetic Models

Capitalizing on the synthetic achievements described in the previous sections, in conjunction with the elucidation of the sequential EnT and ET photoinduced processes in their $\text{ZnP}-[\text{Cu}(\text{phen})_2]^+-\text{C}_{60}$ interlocked molecules, Megiato and Schuster decided to explore rotaxane architectures as molecular platforms to position several chromophores in space. The idea was to promote a cascade of directional and short range photoinduced EnT and ET processes among the interlocked chromophores to ultimately yield long-living CSSs as already observed by Moore, Moore and Gust in their covalently linked D-A systems [78,79,100–106]. By combining the $[\text{Cu}(\text{phen})_2]^+$ -based stepwise template technique, ester reactions and “click” chemistry, the authors developed a synthetic tactic to prepare $[\text{Cu}(\text{phen})_2]^+$ -based rotaxanes with distinct chromophores as stoppers (Figure 13). Accordingly, the strategy relied on a sequential “stoppering–threading–stoppering” approach. The hydroxyl group in phen-thread **23** was esterified with Zn(II)porphyrinate **22** using the EDC/DMAP coupling agent system to afford phen derivative **24**. Threading of **24** through the C_{60} -based macrocycle by means of Sauvage’s Cu(I) template technique quantitatively yielded monostoppered pseudorotaxane **25**, which was allowed to react with either alkynyl ferrocene or ethynyl Zn(II)phtalocyanine (ZnPc) under “click” conditions to produce the target multichromophoric rotaxanes **26** and **27** (Figure 13) [107].

A thorough investigation of the excited states’ properties and decay processes by steady state and time resolved emission spectroscopies, as well as transient absorption techniques, was carried out by Guldi’s group to reveal the photophysical properties of the new multichromophoric rotaxanes. Figure 14 shows the energy level diagrams that summarize the sequence and rate constants of the photophysical events occurring upon excitation of the mechanically linked chromophores. In the case of rotaxane **26** (Figure 14a), it was found that excitation of the ZnP group triggered the expected sequence of EnT and ET processes (steps 1, 3 and 4) to yield the $\text{Fc}-\text{ZnP}^{\bullet+}-[\text{Cu}(\text{phen})_2]^+-\text{C}_{60}^{\bullet-}$ CSS with a lifetime of 2.3 μs , which was much longer than that observed for the same CSS in the parent $(\text{ZnP})_2-[\text{Cu}(\text{phen})_2]^+-\text{C}_{60}$ rotaxane **18** (0.24 μs). That was a surprising result as it was expected on thermodynamic grounds that the Fc stopper would rapidly quench the $\text{ZnP}^{\bullet+}$ via a charge shift reaction (step 6) to afford the final $\text{Fc}^{\bullet+}-\text{ZnP}-[\text{Cu}(\text{phen})_2]^+-\text{C}_{60}^{\bullet-}$ CSS. Such a finding suggested that rotaxane **26** was also conformationally flexible. However, structural investigation by NMR spectroscopy to identify possible rotaxane conformations was unsuccessful, as unsymmetrical rotaxane **26** yielded interpretable NMR spectra in different solvents and temperatures. Fortunately, transient absorption spectra

clearly revealed formation of the final $\text{Fc}^{\bullet+}\text{-ZnP-}[\text{Cu}(\text{phen})_2]^+\text{-C}_{60}^{\bullet-}$ CSS in rotaxane **26**, which mainly occurred from direct ET from the Fc stopper to the oxidized $[\text{Cu}(\text{phen})_2]^{2+}$ complex (step 5). The lifetime of the $\text{Fc}^{\bullet+}\text{-ZnP-}[\text{Cu}(\text{phen})_2]^+\text{-C}_{60}^{\bullet-}$ CSS was 61 μs , which remains the longest lifetime ever detected in interlocked structures [107].

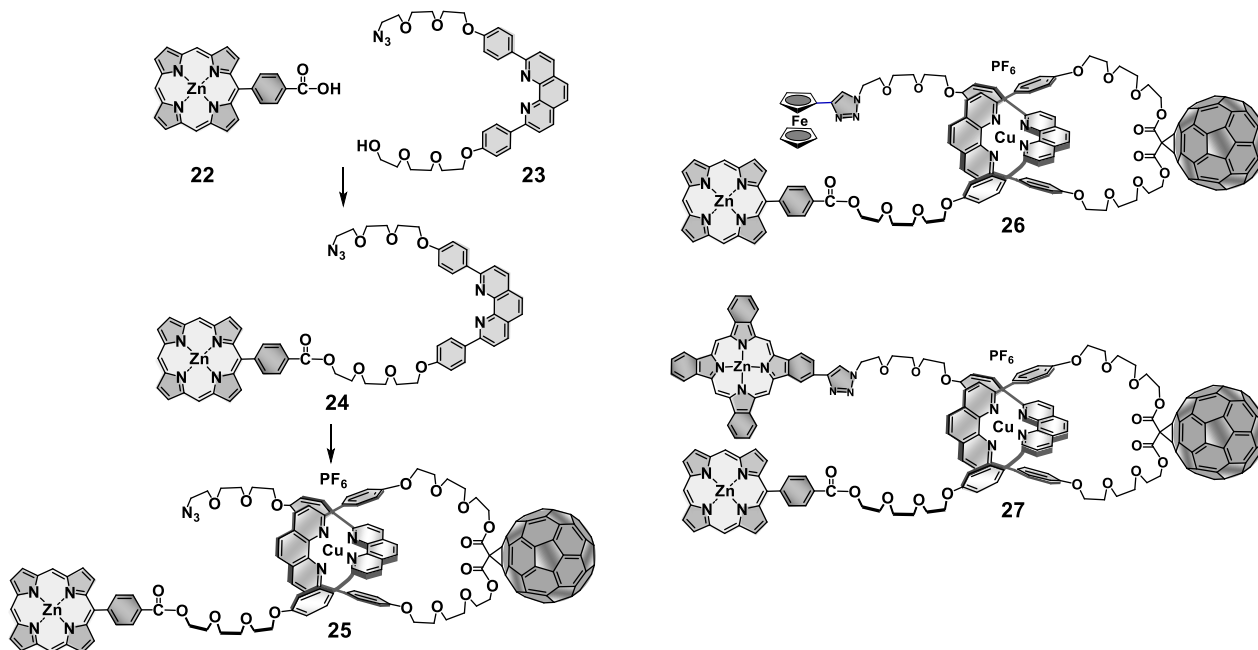


Figure 13. Stopping–threading–stopping synthetic strategy for the synthesis of multi-chromophoric rotaxanes **26** and **27**. Butylphenyl groups located at the periphery of the porphyrin and phthalocyanine moieties are not shown for clarity purposes.

Regarding rotaxane **27**, excitation of the ZnP stopper led to singlet-to-singlet EnT to the ZnPc moiety (step 1) in competition with intersystem crossing to produce $^3\text{ZnP}^*$ and $^3\text{ZnPc}^*$ (steps 2 and 3). The $^1\text{ZnPc}^*$ manifold decayed via EnT to the $[\text{Cu}(\text{phen})_2]^+$ complex to produce the $^3\text{MLCT}^*$ (step 4), which in turn decayed via ET to the fullerene acceptor to yield the intermediate $\text{ZnP-ZnPc-}[\text{Cu}(\text{phen})_2]^{2+}\text{-C}_{60}^{\bullet-}$ CSS (step 5). A charge shift reaction from the ZnPc to the oxidized $[\text{Cu}(\text{phen})_2]^{2+}$ complex occurred (step 6) followed by a second charge shift reaction from the ZnP to the $\text{ZnPc}^{\bullet+}$ radical cation (step 7) to yield the final $\text{ZnP}^{\bullet+}\text{-ZnPc-}[\text{Cu}(\text{phen})_2]^{2+}\text{-C}_{60}^{\bullet-}$ CSS with a lifetime of 8.4 μs . The observed shorter lifetime of the final CSS in rotaxane **27** when compared to that of **26** was most likely due to the ZnP, $[\text{Cu}(\text{phen})_2]^+$ complex and ZnPc centered CSSs being energetically at a similar levels in rotaxane **27** (1.31. eV), while the Fc centered CSS was energetically favored (1.10 eV) in rotaxane **26**. With those findings, Megiatto, Schuster and Guldi demonstrated that rotaxanes are useful molecular platforms to assemble several chromophores which are able to absorb light over a very wide range of the visible region, triggering a cascade of short-range EnT and ET processes to afford long-lived charge-separated states [107].

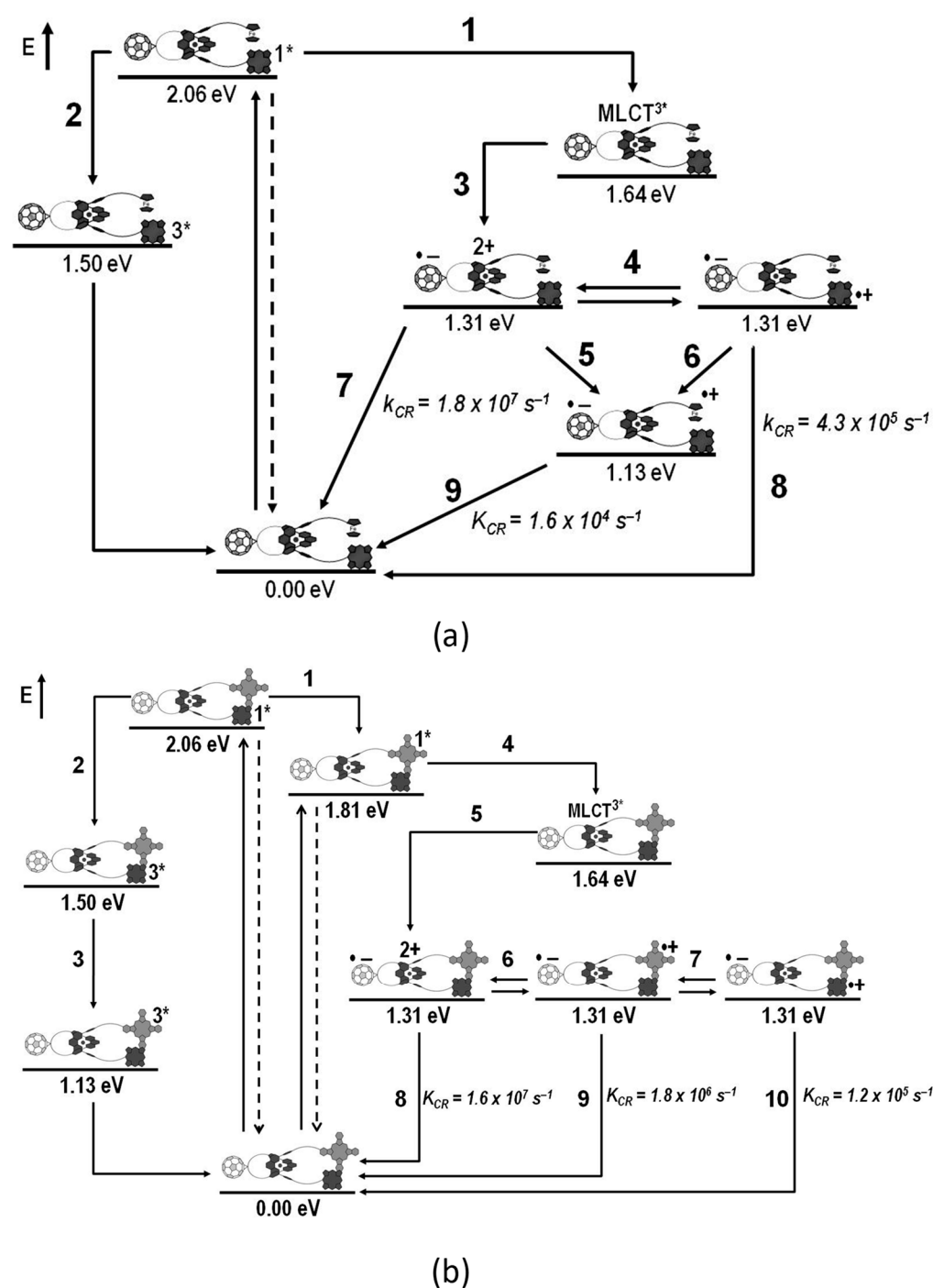


Figure 14. Energy level diagrams, proposed decay pathways, and rate constants in s^{-1} following exclusive excitation of the ZnP subunit at 425 nm: (a) rotaxane 26; (b) rotaxane 27.

6. Active-Metal Template Synthesis of Photoactive Rotaxanes

There is a significant amount of literature on the transition metal template synthesis of interlocked molecules. Despite the richness of techniques available, complexes and geometries other than the tetrahedral $[\text{Cu}(\text{phen})_2]$ complex have not yet been fully explored in the synthesis of D-A mechanically linked systems [22,108]. However, few examples of D-A rotaxanes have been published recently, in which the interlocked systems are assembled via what has been called active metal template synthesis (AMT). The AMT technique has been popularized by Leigh and coworkers, who, in a series of elegant and influential studies, established the basis to explore the catalytic properties of transition metal ions

rather than relying solely on the coordinative ones [22]. Accordingly, the metal ions not only organize the building blocks in an entwined arrangement but also actively promote the reaction that covalently captures the interlocked structure. The AMT tactic has proven to be a more powerful synthetic approach to assemble interlocked molecules [109–119] and impressive molecular machines, pumps and synthesizers [120–124].

In the field of mechanically linked artificial photosynthetic models, one elegant study by Weiss, Hyashi and Guldi groups has been recently published, in which the ZnP–C₆₀ rotaxane was assembled by the AMT technique (Figure 15) [125]. Specifically, treatment of a ZnP(II)porphyrinate-based macrocycle with [Cu(MeCN)₄][PF₆]⁻ led to formation of bimetallic complex **28**, in which the appended bidentate phen moiety sequesters and positions the Cu(I) ion inside the cavity of the macrocycle. As Cu(I) ions are the promoters of “click reactions”, complex **28** is an endotopic catalyst that in the presence of alkynyl fullerene **29** and azide stopper **30** promotes the “click reaction” through the macrocycle cavity to yield target rotaxane **31** in 48% yield, after removal of the Cu(I) ions with EDTA. From structural investigations, the authors demonstrated that the resulting triazole ring on the thread was coordinated to the Zn(II) ion in the porphyrin core. This intracomponent interaction fixes the position of the fullerene stopper at about 5.6 Å to the ZnP moiety in rotaxane **31** (according to computational calculations) and prevents the shuttling movement of the ring along the thread.

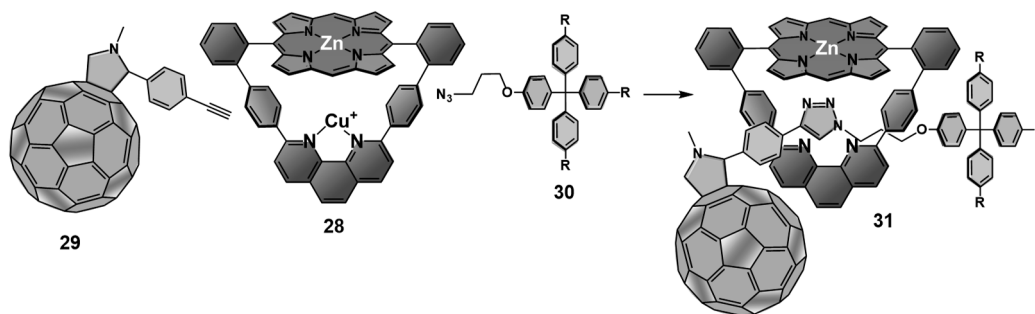


Figure 15. Active metal template synthesis of rotaxane **31** developed by Weiss’ and Guldi’s groups.

The authors found that the photophysical decay of rotaxane **31** was dependent of the solvent polarity. In apolar toluene, excitation of the ZnP group yielded the ¹ZnP*, which decayed through ET to the C₆₀ to generate the ZnP^{•+}–C₆₀^{•-} CSS, and via intersystem crossing to produce the ³ZnP* manifold. The lifetime of the CSS in toluene was 12.8 ns, informing the authors that the ZnP group on the ring was anchored to the triazole moiety on the thread. Interestingly, in polar benzonitrile a short-lived (1.77 ns) and a long-lived (9.42 ns) CSSs were detected. The authors proposed that photooxidation of the ZnP by ET to the fullerene resulted in distortions of the ZnP scaffold, which in turn led to de-coordination of the triazole ring on the thread to allow benzonitrile solvent molecules to coordinate to the Zn(II) ion. Such a process allowed the ring to randomly move along the thread, thereby changing the distance between the chromophores to cause the observed biexponential decay of the ZnP^{•+}–C₆₀^{•-} CSS. Amusingly, it was found that the coordination of pyridine to ZnP group led to directional motion of the ring about the thread when the rotaxane was dissolved in apolar toluene, which brought the ZnP^{•+} closer to the C₆₀^{•-}. Consequently, the lifetime of the ZnP^{•+}–C₆₀^{•-} CSS was biexponential in toluene, with lifetimes of 1.7 ns (major component) and 9.42 ns (minor component, corresponding to the fraction of rotaxanes in which the ZnP group was still anchored to the triazole moiety). Thus, this work demonstrated that formation of coordinative bonds can drive directional intercomponent motion in rotaxanes to influence the photoinduced processes in D-A interlocked systems.

Anderson’s group has also reported a series of complex photoactive interlocked structures [126–129]. In one of their designs [130], polyyn rotaxane **33** was assembled via the AMT technique (Figure 16). Phen-based macrocycle **32** is an endotopic catalyst for

alkyne–alkyne coupling, which connects the stoppers together in an interlocked fashion to yield **33** in 65% yield, after removal of the Cu(I) ion. Due to the coordinating nature of the bidentate phen moiety, the authors also explored the rotaxane environment to position Re(I) complexes, which are highly luminescent, near the hexayne chain to form rotaxane **34**. However, the luminescence of the Re(I) complex in **34** was totally quenched, which was a surprising finding as the HOMO-LUMO gap and the electron affinity of the polyyne chain were insufficient to thermodynamically allow EnT and ET processes between the components of rotaxane **34**.

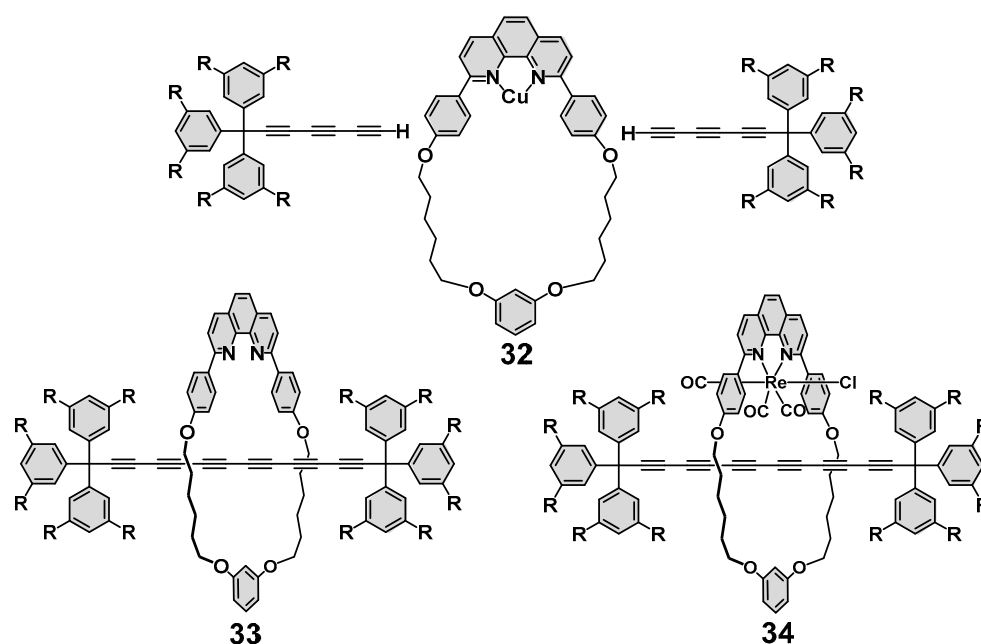


Figure 16. Active metal template synthesis of polyyne rotaxanes developed by Anderson's group.

A thoroughly spectroscopic investigation associated with time-dependent Density Functional Calculations (TD-DFT) revealed the reasons for the unexpected luminescence quenching of the Re(I) complex in **34**. Using ultrafast UV-NIR pump-probe transient absorption spectroscopy, it was found that a rapid triplet energy migration from the $^3\text{MLCT}^*$ excited state centered at the Re(I) complex to the thread hexayne occurred with a time constant of 1.5 ns. To understand the decay processes of the excited states on the polyyne thread, the authors investigated metal free rotaxane **33** by time-resolved infrared spectroscopy. Following the $\text{C}\equiv\text{C}$ stretching frequencies ($2100\text{--}2200\text{ cm}^{-1}$) upon irradiation, it was found that the polyyne excited states (S_n , S_1 and T_1) had a significant cumulenic character, i.e., the $\text{C}\equiv\text{C}$ triple bonds became longer and $\text{C}\text{--}\text{C}$ bonds became shorter. The X-ray crystal structure of **34** revealed that the $\text{Re}(\text{CO})_3\text{Cl}$ center and the hexayne chain were in close contact, with the latter bending around the former. The authors concluded that such close contact caused the observed through-space electronic perturbation on both components in the excited state. This elegant work demonstrated the usefulness of rotaxane structures for investigating complex electronic excited interactions that would be rather difficult, if not impossible, to study with non-interlocked compounds [130].

7. Conclusions

This brief account concerning photoactive interlocked molecules assembled by transition metal template techniques describes major advances in the field over more than 30 years of research work. As one can see, mechanically linked D-A systems offer many advantages over D-A covalently linked analogs. Key parameters that are believed to be critical in natural photosynthesis, such as molecular topology and conformational changes of the photoactive subunits in the protein array upon photoexcitation, can be mimicked and

better understood using photoactive interlocked molecules. Furthermore, the possibility of controlling the direction of the component molecular motions via external stimuli or stabilizing elusive intermediates renders those interactive photoactive systems very promising to further improve our understanding of ET and EnT processes. With the continuous advance of ultrafast spectroscopic techniques associated with the huge number of template synthetic tactics that can be used to prepare D-A interlocked molecules, we can safely conclude that this field has bright future.

Funding: This research was funded by Fundação de Amparo à Pesquisa do Estado de São Paulo (FAPESP), grant number 2013/22160-0 and by Conselho Nacional de Desenvolvimento Científico e Tecnológico (CNPq), grant number 307635/2018-0.

Institutional Review Board Statement: Not applicable.

Informed Consent Statement: Not applicable.

Conflicts of Interest: The authors declare no conflict of interest.

References

1. Burns, C.J.; Stoddart, J.F. *The Nature of the Mechanical Bond: From Molecules to Machines*; John Wiley & Sons, Inc.: Hoboken, NJ, USA, 2017.
2. Stoddart, J.F. Mechanically Interlocked Molecules (MIMs)-Molecular Shuttles, Switches, and Machines (Nobel Lecture). *Angew. Chem. Int. Ed.* **2017**, *56*, 11094–11125. [[CrossRef](#)]
3. Stoddart, J.F. The chemistry of the mechanical bond. *Chem. Soc. Rev.* **2009**, *38*, 1802–1820. [[CrossRef](#)] [[PubMed](#)]
4. Sauvage, J.-P. From Chemical Topology to Molecular Machines (Nobel Lecture). *Angew. Chem. Int. Ed.* **2017**, *56*, 11080–11093. [[CrossRef](#)] [[PubMed](#)]
5. Sauvage, J.-P. Interlacing molecular threads on transition metals: Catenands, catenates, and knots. *Acc. Chem. Res.* **1990**, *23*, 319–327. [[CrossRef](#)]
6. Erbas-Cakmak, S.; Leigh, D.A.; McTernan, C.T.; Nussbaumer, A.L. Artificial Molecular Machines. *Chem. Rev.* **2015**, *18*, 10081–10206. [[CrossRef](#)] [[PubMed](#)]
7. Kassem, S.; van Leeuwen, T.; Lubbe, A.S.; Wilson, M.R.; Feringa, B.L.; Leigh, D.A. Artificial Molecular Motors. *Chem. Soc. Rev.* **2017**, *46*, 2592–2621. [[CrossRef](#)] [[PubMed](#)]
8. Dietrich-Buchecker, C.O.; Sauvage, J.-P. Interlocking of molecular threads: From the statistical approach to the templated synthesis of catenands. *Chem. Rev.* **1987**, *87*, 795–810. [[CrossRef](#)]
9. Lehn, J.-M. *Supramolecular Chemistry: Concepts and Perspectives*, 1st ed.; Wiley-VCH: Weinheim, Germany, 1995.
10. Raymo, F.M.; Stoddart, J.F. Templated synthesis of catenanes and rotaxanes. In *Templated Organic Synthesis*; Diederich, F., Stang, P.J., Eds.; Wiley-VCH Verlag GmbH: Weinheim, Germany, 2000; pp. 75–104.
11. Fujita, M. Metal-directed self-assembly of two- and three-dimensional synthetic receptors. *Chem. Soc. Rev.* **1998**, *27*, 417–425. [[CrossRef](#)]
12. Vögtle, F.; Dünnwald, T.; Schmidt, T. Catenanes and Rotaxanes of the Amide Type. *Acc. Chem. Res.* **1996**, *29*, 451–460. [[CrossRef](#)]
13. Crowley, J.D.; Goldup, S.M.; Lee, A.-L.; Leigh, D.A.; McBurney, R.T. Active metal template synthesis of rotaxanes, catenanes and molecular shuttles. *Chem. Soc. Rev.* **2009**, *38*, 1530–1541. [[CrossRef](#)]
14. Schalley, C.A.; Vögtle, F.; Dötz, K.H. *Templates in Chemistry*; Springer: Berlin, Germany, 2004; Volumes 1 and 2.
15. Roche, C.; Sour, A.; Sauvage, J.-P. A Flexible Copper(I)-Complexed [4]Rotaxane Containing Two Face-to-Face Porphyrinic Plates that Behaves as a Distensible Receptor. *Chem. Eur. J.* **2012**, *18*, 8366–8376. [[CrossRef](#)]
16. Saalfrank, R.W.; Bernt, I. Ligand and metal controlled multicomponent self-assembly of oligonuclear two- and three-dimensional complex molecular architectures. *Curr. Opin. Solid State Mater. Sci.* **1998**, *3*, 407–413. [[CrossRef](#)]
17. Saalfrank, R.W.; Bernt, I.; Ullmer, E.; Hampel, F. Template-mediated self-assembly of six- and eight membered iron coronates. *Angew. Chem. Int. Ed.* **1997**, *36*, 2482–2495. [[CrossRef](#)]
18. Sauvage, J.P. *Transition Metals in Supramolecular Chemistry*; John Wiley & Sons, Inc.: Chichester, UK, 2008; Volume 5.
19. Dietrich-Buchecker, C.O.; Sauvage, J.P.; Kintzinger, J.P. New family of molecules: The metallo-catenanes. *Tetrahedron Lett.* **1983**, *24*, 5095–5098. [[CrossRef](#)]
20. Beves, J.E.; Blight, B.A.; Campbell, C.J.; Leigh, D.A.; McBurney, R.T. Strategies and Tactics for the Metal-Directed Synthesis of Rotaxanes, Knots, Catenanes, and Higher Order Links. *Angew. Chem. Int. Ed.* **2011**, *50*, 9260–9327. [[CrossRef](#)]
21. Schmittel, M.; Ganz, A. Stable mixed phenanthroline copper (i) complexes. Key building blocks for supramolecular coordination chemistry. *Chem. Commun.* **1997**, *11*, 999–1000. [[CrossRef](#)]
22. Saha, M.L.; Neogi, S.; Schmittel, M. Dynamic heteroleptic metal-phenanthroline complexes: From structure to function. *Dalton Trans.* **2014**, *43*, 3815–3834. [[CrossRef](#)] [[PubMed](#)]
23. Wasielewski, M.R. Photoinduced electron transfer in supramolecular systems for artificial photosynthesis. *Chem. Rev.* **1992**, *92*, 435–461. [[CrossRef](#)]

24. Balzani, V. *Supramolecular Photochemistry*; Springer: Heidelberg, Germany, 1987.
25. Balzani, V. *Supramolecular Photochemistry*. *Tetrahedron* **1992**, *48*, 10443–10514. [[CrossRef](#)]
26. Chambron, J.-C.; Collin, J.-P.; Dalbavie, J.-O.; Dietrich-Buchecker, C.O.; Heitz, V.; Odobel, F.; Solladie, N.; Sauvage, J.-P. Rotaxanes and other transition metal-assembled porphyrin arrays for long-range photoinduced charge separation. *Coord. Chem. Rev.* **1998**, *178–180 Pt 2*, 1299–1312. [[CrossRef](#)]
27. Benniston, A.C. Photo- and redox-active [2]rotaxanes and [2]catenanes. *Chem. Soc. Rev.* **1996**, *25*, 427–435. [[CrossRef](#)]
28. Segura, J.L.; Martin, N. New concepts in tetrathiafulvalene chemistry. *Angew. Chem. Int. Ed.* **2001**, *40*, 1372–1409. [[CrossRef](#)]
29. Armaroli, N. Photoactive mono- and polynuclear Cu(I)-phenanthrolines. A viable alternative to Ru (II)-polypyridines? *Chem. Soc. Rev.* **2001**, *30*, 113–124. [[CrossRef](#)]
30. Balzani, V.; Credi, A.; Raymo, F.M.; Stoddart, J.F. Artificial molecular machines. *Angew. Chem. Int. Ed.* **2000**, *39*, 3348–3391. [[CrossRef](#)]
31. Diederich, F.; Gomez-Lopez, M. Supramolecular fullerene chemistry. *Chem. Soc. Rev.* **1999**, *28*, 263–277. [[CrossRef](#)]
32. Meichsner, E.; Nierengarten, I.; Holler, M.; Chessé, M.; Nierengarten, J.-F. A fullerene-substituted pillar [5]arene for the construction of a photoactive rotaxane. *Helv. Chim. Acta* **2018**, *101*, e1800059. [[CrossRef](#)]
33. Steffenhagen, M.; Latus, A.; Trinh, T.M.N.; Nierengarten, I.; Lucas, I.T.; Joiret, S.; Landoulsi, J.; Delavaux-Nicot, B.; Nierengarten, J.-F.; Maisonhaute, E. A rotaxane scaffold bearing multiple redox centers: Synthesis, surface modifications and electrochemical properties. *Chem. Eur. J.* **2018**, *24*, 1701–1708. [[CrossRef](#)] [[PubMed](#)]
34. Delavaux-Nicot, B.; Ben Aziza, H.; Nierengarten, I.; Trinh, T.M.N.; Meichsner, E.; Chessé, M.; Holler, M.; Abadi, R.; Maisonhaute, E.; Nierengarten, J.-F. A rotaxane scaffold for the construction of multiporphyrinic light-harvesting devices. *Chem. Eur. J.* **2018**, *24*, 133–140. [[CrossRef](#)] [[PubMed](#)]
35. de Juan, A.; Pouillon, Y.; Ruiz-Gonzalez, L.; Torres-Pardo, A.; Casado, S.; Martin, N.; Rubio, A.; Perez, E.M. Mechanically Interlocked Single-Wall Carbon Nanotubes. *Angew. Chem. Int. Ed.* **2014**, *53*, 5394–5400. [[CrossRef](#)] [[PubMed](#)]
36. Barrejon, M.; Mateo-Alonso, A.; Prato, M. Carbon Nanostructures in Rotaxane Architectures. *Eur. J. Org. Chem.* **2019**, *21*, 3371–3383. [[CrossRef](#)]
37. Martinez-Diaz, M.V.; Fender, N.S.; Rodriguez-Morgade, M.S.; Gomez-Lopez, M.; Diederich, F.; Echegoyen, L.; Stoddart, J.-F.; Torres, T. A Supramolecular Approach for The Formation of Fullerene–Phthalocyanine Dyads. *J. Mat. Chem.* **2002**, *12*, 2095–2099. [[CrossRef](#)]
38. Guldi, D.M.; Ramey, J.; Martinez-Diaz, M.V.; de la Escosura, A.; Torres, T.; Da Ros, T.; Prato, M. Reversible Zinc Phthalocyanine Fullerene Ensembles. *Chem. Commun.* **2002**, *23*, 2774–2775. [[CrossRef](#)]
39. Diaz, M.C.; Illescas, M.; Martin, N.; Stoddart, J.-F.; Canales, M.A.; Jimenez-Barbero, J.; Sarova, G.; Guldi, D.M. Supramolecular pseudo-rotaxane type complexes from π -extended TTF dimer crown ether and C₆₀. *Tetrahedron* **2006**, *62*, 1998–2002. [[CrossRef](#)]
40. Illescas, B.M.; Santos, J.; Diaz, M.C.; Martin, N.; Atienza, C.M.; Guldi, D.M. Supramolecular Threaded Complexes from Fullerene–Crown Ether and π -Extended TTF Derivatives. *Eur. J. Org. Chem.* **2007**, *30*, 5027–5037. [[CrossRef](#)]
41. Watanabe, N.; Kihara, N.; Furusho, Y.; Takata, T.; Araki, Y.; Ito, O. Photoinduced Intrarotaxane Electron Transfer between Zinc Porphyrin and [60]Fullerene in Benzonitrile. *Angew. Chem. Int. Ed.* **2003**, *42*, 681–683. [[CrossRef](#)] [[PubMed](#)]
42. Da Ros, T.; Guldi, D.M.; Morales, A.F.; Leigh, D.A.; Prato, M.; Turco, R. Hydrogen Bond-Assembled Fullerene Molecular Shuttle. *Org. Lett.* **2003**, *5*, 689–691. [[CrossRef](#)]
43. Mateo-Alonso, A.; Ehli, C.; Rahman, G.M.A.; Guldi, D.M.; Fioravanti, G.; Marcaccio, M.; Paolucci, M.; Prato, M. Tuning Electron Transfer through Translational Motion in Molecular Shuttles. *Angew. Chem. Int. Ed.* **2007**, *46*, 3521–3525. [[CrossRef](#)]
44. Mateo-Alonso, A.; Iliopoulos, K.; Couris, S.; Prato, M. Charge Transfer Reactions along a Supramolecular Redox Gradient. *J. Am. Chem. Soc.* **2008**, *130*, 14938–14939. [[CrossRef](#)]
45. Saha, S.; Flood, A.H.; Stoddart, J.-F.; Impellizzeri, S.; Silvi, S.; Venturi, M.; Credi, A. A Redox-Driven Multicomponent Molecular Shuttle. *J. Am. Chem. Soc.* **2007**, *129*, 12159–12171. [[CrossRef](#)]
46. Ashton, P.R.; Diederich, F.; Gomez-Lopez, M.; Nierengarten, J.-F.; Preece, J.A.; Raymo, F.M.; Stoddart, J.F. Self-Assembly of the First Fullerene-Containing [2]Catenane. *Angew. Chem. Int. Ed.* **1997**, *36*, 1448–1451. [[CrossRef](#)]
47. Nakamura, Y.; Minami, S.; Lizuka, K.; Nishimura, J. Preparation of Neutral [60]Fullerene-Based [2]Catenanes and [2]Rotaxanes Bearing an Electron-Deficient Aromatic Diimide Moiety. *Angew. Chem. Int. Ed.* **2003**, *42*, 3158–3162. [[CrossRef](#)] [[PubMed](#)]
48. Ngo, H.T.; Lewis, J.E.M.; Payne, D.T.; D’Souza, F.; Hill, J.P.; Ariga, K.; Yoshikawa, G.; Goldup, S.M. Rotaxanation as a sequestering template to preclude incidental metal insertion in complex oligochromophores. *Chem. Commun.* **2020**, *56*, 7447–7450. [[CrossRef](#)] [[PubMed](#)]
49. Yamada, Y.; Kato, T.; Tanaka, K. Assembly of Multi-Phthalocyanines on a Porphyrin Template by Four fold Rotaxane Formation. *Chem. Eur. J.* **2006**, *22*, 12371–12380. [[CrossRef](#)]
50. Barendt, T.A.; Rašović, I.; Lebedeva, M.A.; Farrow, G.A.; Auty, A.; Chekulaev, D.; Sazanovich, I.V.; Weinstein, J.A.; Porfyrakis, K.; Beer, P.D. Anion-Mediated Photophysical Behavior in a C₆₀ Fullerene [3]Rotaxane Shuttle. *J. Am. Chem. Soc.* **2018**, *140*, 1924–1936. [[CrossRef](#)]
51. Colasson, B.; Credi, A.; Ventura, B. Photoinduced Electron Transfer Involving a Naphthalimide Chromophore in Switchable and Flexible [2]Rotaxanes. *Chem. Eur. J.* **2020**, *26*, 534–542. [[CrossRef](#)] [[PubMed](#)]
52. Xu, Y.; Kaur, R.; Wang, B.; Minameyer, M.B.; Gsänger, S.; Meyer, B.; Drewello, T.; Guldi, D.M.; von Delius, M. Concave–Convex π – π Template Approach Enables the Synthesis of [10]Cycloparaphenylene–Fullerene [2]Rotaxanes. *J. Am. Chem. Soc.* **2018**, *140*, 13413–13420. [[CrossRef](#)]

53. Browne, C.; Ronson, T.K.; Nitschke, J.R. Palladium-Templated Subcomponent Self-Assembly of Macrocycles, Catenanes, and Rotaxanes. *Angew. Chem. Int. Ed.* **2014**, *53*, 10701–10705. [[CrossRef](#)]
54. Alstrum-Acevedo, J.H.; Brennaman, M.K.; Meyer, T.J. Chemical Approaches to Artificial Photosynthesis. 2. *Inorg. Chem.* **2005**, *44*, 6802–6827. [[CrossRef](#)]
55. Flamigni, L.; Collin, J.-P.; Sauvage, J.-P. Iridium Terpyridine Complexes as Functional Assembling Units in Arrays for the Conversion of Light Energy. *Acc. Chem. Res.* **2008**, *41*, 857–871. [[CrossRef](#)]
56. Hewson, S.W.; Mullen, K.M. Porphyrin-Containing Rotaxane Assemblies. *Eur. J. Org. Chem.* **2019**, *21*, 3358–3370. [[CrossRef](#)]
57. Flamigni, L. Photoinduced processes in interlocked structures containing porphyrins. *J. Photochem. Photobiol. C Photochem. Rev.* **2007**, *8*, 191–210. [[CrossRef](#)]
58. Megiatto, J.D., Jr.; Guldi, D.M.; Schuster, D.I. *Fullerenes: Principles and Applications*; de la Puente, F.L., Nierengarten, J.F., Eds.; Royal Society of Chemistry: Cambridge, UK, 2012; Volume 1, Chapter 10.
59. Chambron, J.-C.; Heitz, V.; Sauvage, J.-P. Transition metal templated formation of [2]- and [3]-rotaxanes with porphyrins as stoppers. *J. Am. Chem. Soc.* **1993**, *115*, 12378–12384. [[CrossRef](#)]
60. Chambron, J.-C.; Harriman, A.; Heitz, V.; Sauvage, J.-P. Ultrafast photoinduced electron transfer between porphyrinic subunits within a bis (porphyrin)-stopped rotaxane. *J. Am. Chem. Soc.* **1993**, *115*, 6109–6114. [[CrossRef](#)]
61. Linke, M.; Chambron, J.-C.; Heitz, V.; Sauvage, J.-P. Electron transfer between mechanically linked porphyrins in a [2]rotaxane. *J. Am. Chem. Soc.* **1997**, *119*, 11329–11330. [[CrossRef](#)]
62. Linke, M.; Chambron, J.-C.; Heitz, V.; Semetey, V. Complete rearrangement of a multi-porphyrinic rotaxane by metallation–demetallation of the central coordination site. *Chem. Commun.* **1998**, *23*, 2469–2470. [[CrossRef](#)]
63. Solladié, N.; Chambron, J.-C.; Sauvage, J.-P. Porphyrin-stoppered [3]- and [5]-rotaxanes. *J. Am. Chem. Soc.* **1999**, *121*, 3684–3692. [[CrossRef](#)]
64. Andersson, M.; Linke, M.; Chambron, J.C.; Davidsson, J.; Heitz, V.; Sauvage, J.-P.; Hammarström, L. Porphyrin-containing [2]-rotaxanes: Metal coordination enhanced superexchange electron transfer between noncovalently linked chromophores. *J. Am. Chem. Soc.* **2000**, *122*, 3526–3527. [[CrossRef](#)]
65. Flamigni, L.; Armaroli, N.; Barigelletti, F.; Chambron, J.-C.; Sauvage, J.-P.; Solladié, N. Photoinduced processes in porphyrin-stoppered [3]-rotaxanes. *New J. Chem.* **1999**, *23*, 1151–1158. [[CrossRef](#)]
66. Linke, M.; Heitz, V.; Sauvage, J.-P.; Encinas, S.; Barigelletti, F.; Flamigni, L. Multiporphyrinic rotaxanes: Control of intramolecular electron transfer rate by steering the mutual arrangement of the chromophores. *J. Am. Chem. Soc.* **2000**, *122*, 11834–11844. [[CrossRef](#)]
67. Andersson, M.; Linke, M.; Chambron, J.C.; Davidsson, J.; Heitz, V.; Hammarström, L.; Sauvage, J.-P. Long-range electron transfer in porphyrin-containing [2]-rotaxanes: Tuning the rate by metal cation coordination. *J. Am. Chem. Soc.* **2002**, *124*, 4347–4362. [[CrossRef](#)]
68. Flamigni, L.; Talarico, A.M.; Chambron, J.C.; Heitz, V.; Linke, M.; Fujita, N.; Sauvage, J.-P. Photoinduced Electron Transfer in Multiporphyrinic Interlocked Structures: The Effect of Copper (i) Coordination in the Central Site. *Chem. Eur. J.* **2004**, *10*, 2689–2699. [[CrossRef](#)] [[PubMed](#)]
69. Flamigni, L.; Heitz, V.; Sauvage, J.-P. Porphyrin Rotaxanes and Catenanes: Copper (I)-Templated Synthesis and Photoinduced Processes. In *Non-Covalent Multi-Porphyrin Assemblies*; Alessio, E., Ed.; Springer: Berlin/Heidelberg, Germany, 2006; pp. 217–261.
70. Guldi, D.M.; Prato, M. Excited-State Properties of C₆₀ Fullerene Derivatives. *Acc. Chem. Res.* **2000**, *33*, 695–703. [[CrossRef](#)]
71. Guldi, D.M. Fullerene–porphyrin architectures; photosynthetic antenna and reaction center models. *Chem. Soc. Rev.* **2002**, *31*, 22–36. [[CrossRef](#)] [[PubMed](#)]
72. Moore, G.F.; Megiatto, J.D., Jr.; Hamburger, M.; Gervaldo, M.; Kodis, G.; Moore, T.A.; Gust, D.; Moore, A.L. Optical and electrochemical properties of hydrogen-bonded phenol-pyrrolidino [60]fullerenes. *Photochem. Photobiol. Sci.* **2012**, *11*, 1018–1025. [[CrossRef](#)]
73. Hirsch, A.; Brettreich, M. *Fullerenes*; Wiley-VCH: Weinheim, Germany, 2005.
74. Schuster, D.I.; Megiatto, J.D., Jr. Nanotubes reveal all in solution. *Nat. Chem.* **2009**, *1*, 182–183. [[CrossRef](#)]
75. Megiatto, J.D., Jr.; Guldi, D.M.; Schuster, D.I. Design, synthesis and photoinduced processes in molecular interlocked photosynthetic [60]fullerene systems. *Chem. Soc. Rev.* **2020**, *49*, 8–20. [[CrossRef](#)]
76. Schuster, D.I.; Jarowski, D.A.; Kirschner, A.N.; Wilson, S.R. Molecular modelling of fullerene–porphyrin dyads. *J. Mater. Chem.* **2002**, *12*, 2041–2047. [[CrossRef](#)]
77. Schuster, D.I.; Li, K.; Guldi, D.M.; Palkar, A.; Echegoyen, L.; Stanisky, C.R.; Cross, J.; Niemi, M.; Tkachenko, N.V.; Lemmetyinen, H. Azobenzene-linked porphyrin-fullerene dyads. *J. Am. Chem. Soc.* **2007**, *129*, 15973–15982. [[CrossRef](#)] [[PubMed](#)]
78. Gust, D.; Moore, T.A.; Moore, A.L. Mimicking Photosynthetic Solar Energy Transduction. *Acc. Chem. Res.* **2001**, *34*, 40–48. [[CrossRef](#)] [[PubMed](#)]
79. Gust, D.; Moore, T.A.; Moore, A.L. Molecular mimicry of photosynthetic energy and electron transfer. *Acc. Chem. Res.* **1993**, *26*, 198–205. [[CrossRef](#)]
80. Marcus, R.A. On the theory of oxidation-reduction reactions involving electron transfer. I. *J. Chem. Phys.* **1956**, *24*, 966–978. [[CrossRef](#)]
81. Diederich, F.; Dietrich-Buchecker, C.O.; Nierengarten, J.-F.; Sauvage, J.-P. A copper (I)-complexed rotaxane with two fullerene stoppers. *Chem. Commun.* **1995**, *7*, 781–782. [[CrossRef](#)]

82. Armaroli, N.; Diederich, F.; Dietrich-Buchecker, C.O.; Flamigni, L.; Marconi, G.; Nierengarten, J.-F.; Sauvage, J.-P. A Copper (I)-Complexed Rotaxane with Two Fullerene Stoppers: Synthesis, Electrochemistry, and Photoinduced Processes. *Chem. Eur. J.* **1998**, *4*, 406–416. [[CrossRef](#)]
83. Li, K.; Schuster, D.I.; Guldi, D.M.; Herranz, M.A.; Echegoyen, L. Convergent Synthesis and Photophysics of [60]Fullerene/Porphyrin-Based Rotaxanes. *J. Am. Chem. Soc.* **2004**, *126*, 3388–3389. [[CrossRef](#)] [[PubMed](#)]
84. Li, K.; Bracher, P.J.; Guldi, D.M.; Herranz, M.A.; Echegoyen, L.; Schuster, D.I. [60]Fullerene-Stoppered Porphyrinorotaxanes: Pronounced Elongation of Charge-Separated-State Lifetimes. *J. Am. Chem. Soc.* **2004**, *126*, 9156–9157. [[CrossRef](#)] [[PubMed](#)]
85. Schuster, D.I.; Li, K.; Guldi, D.M. Porphyrin-fullerene photosynthetic model systems with rotaxane and catenane architectures. *C. R. Chim.* **2006**, *9*, 892–908. [[CrossRef](#)]
86. Meldal, M.; Tornøe, C.W. Cu-Catalyzed Azide–Alkyne Cycloaddition. *Chem. Rev.* **2008**, *108*, 2952–3015. [[CrossRef](#)] [[PubMed](#)]
87. Kolb, C.H.; Finn, M.G.; Sharpless, K.B. Click Chemistry: Diverse Chemical Function from a Few Good Reactions. *Angew. Chem. Int. Ed.* **2001**, *40*, 2004–2021. [[CrossRef](#)]
88. Megiatto, J.D., Jr.; Guldi, D.M.; Schuster, D.I. General method for the synthesis of functionalized macrocycles and catenanes utilizing click chemistry. *J. Am. Chem. Soc.* **2008**, *130*, 12872–12873. [[CrossRef](#)]
89. Megiatto, J.D., Jr.; Spencer, R.; Schuster, D.I. Efficient one-pot synthesis of rotaxanes bearing electron donors and [60]fullerene. *Org. Lett.* **2009**, *11*, 4152–4155. [[CrossRef](#)]
90. Megiatto, J.D., Jr.; Schuster, D.I. Click methodology for the synthesis of functionalized [3]Catenanes: Toward higher interlocked structures. *Chem. A Eur. J.* **2009**, *15*, 5444–5448. [[CrossRef](#)]
91. Megiatto, J.D., Jr.; Schuster, D.I. Introduction of useful peripheral functional groups on [2]catenanes by combining Cu (I) template synthesis with click chemistry. *New J. Chem.* **2010**, *34*, 276–286. [[CrossRef](#)]
92. Megiatto, J.D., Jr.; Schuster, D.I.; Abwandner, S.; de Miguel, G.; Guldi, D.M. [2]Catenanes decorated with porphyrin and [60]fullerene groups: Design, convergent synthesis, and photoinduced processes. *J. Am. Chem. Soc.* **2010**, *132*, 3847–3861. [[CrossRef](#)]
93. Megiatto, J.D., Jr.; Spencer, R.; Schuster, D.I. Optimizing reaction conditions for synthesis of electron donor-[60]fullerene interlocked multiring systems. *J. Mater. Chem.* **2011**, *21*, 1544–1550. [[CrossRef](#)]
94. Megiatto, J.D., Jr.; Schuster, D.I.; de Miguel, G.; Wolfrum, S.; Guldi, D.M. Topological and conformational effects on electron transfer dynamics in porphyrin-[60]fullerene interlocked systems. *Chem. Mater.* **2012**, *24*, 2472–2485. [[CrossRef](#)]
95. Kirner, S.V.; Guldi, D.M.; Megiatto, J.D., Jr.; Schuster, D.I. Synthesis and photophysical properties of new catenated electron donor–acceptor materials with magnesium and free base porphyrins as donors and C₆₀ as the acceptor. *Nanoscale* **2015**, *7*, 1145–1160. [[CrossRef](#)] [[PubMed](#)]
96. Megiatto, J.D., Jr.; Li, K.; Schuster, D.I.; Palkar, A.; Herranz, M.A.; Echegoyen, L.; Abwandner, S.; De Miguel, G.; Guldi, D.M. Convergent synthesis and photoinduced processes in multi-chromophoric rotaxanes. *J. Chem. Phys. B* **2010**, *114*, 14408–14419. [[CrossRef](#)]
97. Jakob, M.; Berg, A.; Levanon, H.; Schuster, D.I.; Megiatto, J.D., Jr. Photoexcited state properties of H₂-porphyrin/C₆₀-based rotaxanes as studied by time-resolved electron paramagnetic resonance spectroscopy. *J. Phys. Chem. A* **2011**, *115*, 5044–5052. [[CrossRef](#)] [[PubMed](#)]
98. Jakob, M.; Berg, A.; Levanon, H.; Schuster, D.I.; Megiatto, J.D., Jr. Photoinduced processes in some mechanically interlocked supramolecules as studied by time-resolved electron paramagnetic resonance. *J. Phys. Chem. C* **2011**, *115*, 24555–24563. [[CrossRef](#)]
99. Megiatto, J.D., Jr.; Schuster, D.I. Alternative demetalation method for Cu (I)-phenanthroline-based catenanes and rotaxanes. *Org. Lett.* **2011**, *13*, 1808–1811. [[CrossRef](#)]
100. Megiatto, J.D., Jr.; Méndez-Hernández, D.D.; Tejada-Ferrari, M.; Teillout, A.-L.; Llansola-Portolés, M.J.; Kodis, G.; Poluektov, O.G.; Rajh, T.; Mujica, V.; Groy, T.L.; et al. A bioinspired redox relay that mimics radical interactions of the tyr-his pairs of photosystem II. *Nat. Chem.* **2014**, *6*, 423–428. [[CrossRef](#)]
101. Antoniuk-Pablant, A.; Terazono, Y.; Brennan, B.J.; Sherman, B.D.; Megiatto, J.D., Jr.; Brudvig, G.W.; Moore, A.L.; Moore, T.A.; Gust, D. A new method for the synthesis of β -cyano substituted porphyrins and their use as sensitizers in photoelectrochemical devices. *J. Mater. Chem. A* **2016**, *4*, 1–10. [[CrossRef](#)]
102. Megiatto, J.D., Jr.; Antoniuk-Pablant, A.; Sherman, B.D.; Kodis, G.; Gervaldo, M.; Moore, T.A.; Moore, A.L.; Gust, D. Mimicking the electron transfer chain in photosystem ii with a molecular triad thermodynamically capable of water oxidation. *Proc. Natl. Acad. Sci. USA* **2012**, *109*, 15578–15583. [[CrossRef](#)]
103. Ravensbergen, J.; Antoniuk-Pablant, A.; Sherman, B.D.; Kodis, G.; Megiatto, J.D., Jr.; Méndez-Hernández, D.D.; Frese, R.N.; Van Grondelle, R.; Moore, T.A.; Moore, A.L.; et al. Spectroscopic analysis of a biomimetic model of Tyr function in PSII. *J. Phys. Chem. B* **2015**, *119*, 12156–12163. [[CrossRef](#)] [[PubMed](#)]
104. Zhao, Y.; Swierk, J.R.; Megiatto, J.D., Jr.; Sherman, B.; Youngblood, W.J.; Qin, D.; Lentz, D.M.; Moore, A.L.; Moore, T.A.; Gust, D.; et al. Improving the efficiency of water splitting in dye-sensitized solar cells by using a biomimetic electron transfer mediator. *Proc. Natl. Acad. Sci. USA* **2012**, *109*, 15612–15616. [[CrossRef](#)] [[PubMed](#)]
105. Megiatto, J.D., Jr.; Patterson, D.; Sherman, B.D.; Moore, T.A.; Gust, D.; Moore, A.L. Intramolecular hydrogen bonding as a synthetic tool to induce chemical selectivity in acid catalyzed porphyrin synthesis. *Chem. Commun.* **2012**, *48*, 4558–4560. [[CrossRef](#)] [[PubMed](#)]

106. Fontana, L.A.; Rigolin, V.H.; Braga, C.B.; Ornelas, C.; Megiatto, J.D., Jr. Methodology for functionalization of water oxidation catalyst IrOx nanoparticles with hydrophobic and multi-functionalized chromophores. *Chem. Commun.* **2021**, *57*, 7398–7401. [[CrossRef](#)] [[PubMed](#)]
107. Kirner, S.V.; Henkel, C.; Guldi, D.M.; Megiatto, J.D., Jr.; Schuster, D.I. Multistep energy and electron transfer processes in novel rotaxane donor-acceptor hybrids generating microsecond-lived charge separated states. *Chem. Sci.* **2015**, *6*, 1–12. [[CrossRef](#)]
108. Chambron, J.-C.; Collin, J.P.; Heitz, V.; Jouvenot, D.; Kern, J.-M.; Mobian, P.; Pomeranc, D.; Sauvage, J.-P. Rotaxanes and Catenanes Built Around Octahedral Transition Metals. *Eur. J. Org. Chem.* **2004**, *8*, 1627–1638. [[CrossRef](#)]
109. Alcantara, A.F.P.; Fontana, L.A.; Rigolin, V.H.; Andrade, Y.S.F.; Ribeiro, M.A.; Barros, W.P.; Ornelas, C.; Megiatto, J.D., Jr. Olefin cyclopropanation via radical carbene transfer reaction promoted by Co (II) porphyrinates for the active-metal-template synthesis of [2]rotaxanes. *Angew. Chem. Int. Ed.* **2018**, *57*, 8979–8983. [[CrossRef](#)]
110. Alcantara, A.F.P.; Fontana, L.A.; Almeida, M.P.; Rigolin, V.H.; Ribeiro, M.A.; Barros, W.P.; Megiatto, J.D., Jr. Control over the Redox Cooperative Mechanism of Radical Carbene Transfer Reactions for the Efficient Active-Metal-Template Synthesis of [2]Rotaxanes. *Chem. Eur. J.* **2020**, *26*, 7808–7822. [[CrossRef](#)] [[PubMed](#)]
111. Fontana, L.A.; Almeida, M.P.; Alcantara, A.F.P.; Rigolin, V.H.; Ribeiro, M.A.; Barros, W.P.; Megiatto, J.D. Ru(II)Porphyrinate-based molecular nanoreactor for carbene insertion reactions and quantitative formation of rotaxanes by active-metal-template syntheses. *Nat. Commun.* **2020**, *11*, 6370. [[CrossRef](#)]
112. Fontana, L.A.; Alcantara, A.F.P.; Rigolin, V.H.; Megiatto, J.D., Jr. Semi-Rigid Ru (II) Porphyrinate-Based Macrocyclic Receptor as Endotopic Catalyst for Carbene Transfer Reactions. *ECS J. Solid State Sci. Technol.* **2020**, *9*, 061023. [[CrossRef](#)]
113. van den Boomen, O.I.; Coumans, R.G.E.; Akeroyd, N.; Peters, T.P.J.; Schlebos, P.P.J.; Smits, J.; de Gelder, R.; Elemans, J.A.A.W.; Nolte, R.J.M.; Rowan, A.E. Carbenoid transfer reactions catalyzed by a ruthenium porphyrin macrocycle. *Tetrahedron* **2017**, *73*, 5029–5037. [[CrossRef](#)]
114. Miyazaki, Y.; Kahlfuss, C.; Ogawa, A.; Matsumoto, T.; Wytko, J.A.; Oohora, K.; Hayashi, T.; Weiss, J. CuAAC in a Distal Pocket: Metal Active-Template Synthesis of Strapped-Porphyrin [2]Rotaxanes. *Chem. Eur. J.* **2017**, *23*, 13579–13582. [[CrossRef](#)]
115. Lewis, J.E.M.; Modicom, F.; Goldup, S.M. Efficient Multi-Component Active Template Synthesis of Catenanes. *J. Am. Chem. Soc.* **2018**, *140*, 4787–4791. [[CrossRef](#)]
116. Denis, M.; Goldup, S.M. The Active Template Approach to Interlocked Molecules: Principles, Progress and Applications. *Nat. Rev. Chem.* **2017**, *1*, 0061. [[CrossRef](#)]
117. Lewis, J.E.M.; Winn, J.; Cera, L.; Goldup, S.M. Iterative Synthesis of Oligo[n]Rotaxanes in Excellent Yield. *J. Am. Chem. Soc.* **2016**, *138*, 16329–16336. [[CrossRef](#)]
118. Acevedo-Jake, A.; Ball, A.T.; Galli, M.; Kukwikila, M.; Denis, M.; Singleton, D.G.; Tavassoli, A.; Goldup, S.M. AT-CuAAC Synthesis of Mechanically Interlocked Oligonucleotides. *J. Am. Chem. Soc.* **2020**, *142*, 5985–5990. [[CrossRef](#)] [[PubMed](#)]
119. Danon, J.J.; Leigh, D.A.; McGonigal, P.R.; Ward, J.W.; Wu, J. Triply-threaded [4]rotaxanes. *J. Am. Chem. Soc.* **2016**, *138*, 12643–12674. [[CrossRef](#)]
120. Thordarson, P.; Bijsterveld, E.J.A.; Rowan, A.E.; Nolte, R.J.M. Epoxidation of polybutadiene by a topologically linked catalyst. *Nature* **2003**, *424*, 915–918. [[CrossRef](#)] [[PubMed](#)]
121. Echavarren, J.; Gall, M.A.Y.; Haertsch, A.; Leigh, D.A.; Spence, J.T.J.; Tetlow, D.J.; Tian, C. Sequence-selective decapeptide synthesis by the parallel operation of two artificial molecular machines. *J. Am. Chem. Soc.* **2021**, *143*, 5158–5165. [[CrossRef](#)]
122. Amano, S.; Fielden, S.D.P.; Leigh, D.A. A catalysis-driven artificial molecular pump. *Nature* **2021**, *594*, 529–534. [[CrossRef](#)]
123. McTernan, C.; De Bo, G.; Leigh, D.A. A track-based molecular synthesizer that builds a single-sequence oligomer through iterative carbon-carbon bond formation. *Chem* **2020**, *6*, 2964–2973. [[CrossRef](#)]
124. Erbas-Cakmak, S.; Fielden, S.D.P.; Karaca, U.; Leigh, D.A.; McTernan, C.T.; Tetlow, D.J.; Wilson, M.R. Rotary and linear molecular motors driven by pulses of a chemical fuel. *Science* **2017**, *358*, 340–343. [[CrossRef](#)] [[PubMed](#)]
125. Wolf, M.; Ogawa, A.; Bechtold, M.; Vonesch, M.; Wytko, J.A.; Oohora, K.; Campidelli, S.; Hayashi, T.; Guldi, D.M.; Weiss, J. Light triggers molecular shuttling in rotaxanes: Control over proximity and charge recombination. *Chem. Sci.* **2019**, *10*, 3846–3853. [[CrossRef](#)]
126. Kohn, D.R.; Movsisyan, L.D.; Thompson, A.L.; Anderson, H.L. Porphyrin-Polyene [3]- and [5]Rotaxanes. *Org. Lett.* **2017**, *19*, 348–351. [[CrossRef](#)]
127. Movsisyan, L.D.; Franz, M.; Hampel, F.; Thompson, A.L.; Tykwinski, R.R.; Anderson, H.L. Polyene Rotaxanes: Stabilization by Encapsulation. *J. Am. Chem. Soc.* **2016**, *138*, 1366–1376. [[CrossRef](#)] [[PubMed](#)]
128. Pruchyathamkorn, J.; Kendrick, W.J.; Frawley, A.T.; Mattioni, A.; Caycedo-Soler, F.; Huelga, S.F.; Plenio, M.B.; Anderson, H.L. A cyanine dye rotaxane porphyrin nanoring complex as a model light harvesting system. *Angew. Chem. Int. Ed.* **2020**, *59*, 16455–16458. [[CrossRef](#)]
129. Movsisyan, L.D.; Kondratuk, D.V.; Franz, M.; Thompson, A.L.; Tykwinski, R.R.; Anderson, A.L. Synthesis of Polyene Rotaxanes. *Org. Lett.* **2012**, *14*, 3424–3426. [[CrossRef](#)]
130. Movsisyan, L.D.; Peeks, M.D.; Greetham, G.M.; Towrie, M.; Thompson, A.L.; Parker, A.W.; Anderson, H.L. Photophysics of Threaded sp-Carbon Chains: The Polyene is a Sink for Singlet and Triplet Excitation. *J. Am. Chem. Soc.* **2014**, *136*, 17996–18008. [[CrossRef](#)] [[PubMed](#)]